

6-1953

Aluminum-vanadium system

D. J. Kenney
Iowa State College

H. A. Wilhelm
Iowa State College

O. N. Carlson
Iowa State College

Follow this and additional works at: http://lib.dr.iastate.edu/ameslab_iscreports



Part of the [Ceramic Materials Commons](#), and the [Metallurgy Commons](#)

Recommended Citation

Kenney, D. J.; Wilhelm, H. A.; and Carlson, O. N., "Aluminum-vanadium system" (1953). *Ames Laboratory ISC Technical Reports*. 51.
http://lib.dr.iastate.edu/ameslab_iscreports/51

This Report is brought to you for free and open access by the Ames Laboratory at Iowa State University Digital Repository. It has been accepted for inclusion in Ames Laboratory ISC Technical Reports by an authorized administrator of Iowa State University Digital Repository. For more information, please contact digirep@iastate.edu.

Aluminum-vanadium system

Abstract

The nature of the aluminum-vanadium system has been reported on the basis of thermal, microscopic, chemical and X-ray evidence. The system contains six different solid phases at ambient temperatures: the four intermediate phase being peritectic in nature. Phase properties are summarized in Table 1.

Keywords

Ames Laboratory

Disciplines

Ceramic Materials | Engineering | Materials Science and Engineering | Metallurgy

UNITED STATES ATOMIC ENERGY COMMISSION

Physical Sciences Reading Room

ISC-353

ALUMINUM-VANADIUM SYSTEM

By

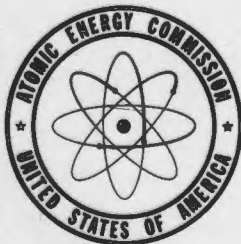
D. J. Kenney

H. A. Wilhelm

O. N. Carlson

June 1953

Ames Laboratory



Technical Information Service, Oak Ridge, Tennessee

UNITED STATES ATOMIC ENERGY COMMISSION
ALUMINUM-VANADIUM SYSTEM
BY
D. J. KENNEY
H. A. WILSON
O. N. CARLSON

METALLURGY AND CERAMICS

This report has been reproduced direct from copy as submitted to the Technical Information Service.

Work performed under
Contract No. W-7405-eng-82.

Arrangements for reproduction of this document in whole or in part should be made directly with the author and the organization he represents. Such reproduction is encouraged by the United States Atomic Energy Commission.

TABLE OF CONTENTS

	Page
I. ABSTRACT.	5
II. INTRODUCTION.	7
III. REVIEW OF LITERATURE.	8
A. Historical Survey.	8
1. Metallography.	8
2. Commercial applications.	11
B. Discussion of Reported Work	13
C. Summary of Pertinent Facts.	13
IV. SOURCE OF MATERIALS	14
A. Aluminum.	14
B. Vanadium.	15
C. Alloys.	15
V. APPARATUS AND METHODS	21
A. Obtaining Thermal Data.	21
B. Annealing the Alloys.	23
C. Preparation of Samples for Microscopic Examination	24
1. Polishing.	24
2. Etching.	25
D. Preparation of Samples for X-Ray Analysis	26
1. Powder specimens	27
2. Solid samples.	27
3. Single crystals.	30
F. Chemical Analysis	31
1. Volumetric	31
2. Spectrophotometric	31
VI. EXPERIMENTAL RESULTS.	31
A. Macroscopic Nature of the System.	31
1. Density.	31
2. Hardness	32
3. Ageing	32

	Page
B. Microscopic Nature of the System	36
1. Introduction.	36
2. Phase properties.	37
(a) (Al).	37
(b) α (Al-V).	37
(c) β (Al-V).	37
(d) γ (Al-V).	39
(e) δ (Al-V).	39
(f) (V).	42
3. Phase relations	45
C. Atomic Nature of the System.	60
1. Introduction.	60
(a) (Al-V).	66
(b) (Al-V).	68
(c) (Al-V).	71
(d) (Al-V).	72
2. Phase transitions	75
VII. DISCUSSION AND SUMMARY	76
VIII. LITERATURE CITED	79

ALUMINUM-VANADIUM SYSTEM*

by

D. J. Kenney, H. A. Wilhelm, and O. N. Carlson

I. ABSTRACT

The nature of the aluminum-vanadium system has been reported on the basis of thermal, microscopic, chemical and X-ray evidence. The system contains six different solid phases at ambient temperatures: the four intermediate phase being peritectic in nature. Phase properties are summarized in Table 1.

The effect of composition upon density can be represented by a series of straight lines; the phase boundaries of the aluminum-vanadium system seem to have some correlation with the discontinuities in slope of these straight lines. The addition of 20 weight per cent aluminum has little effect on the hardness of either as-cast or cold-worked vanadium. All hardness values observed for alloys containing up to 20 per cent by weight aluminum fell within 10 points of 60 on the Rockwell "A" scale. On the other hand, the addition of vanadium to aluminum, has a profound effect on the hardness of the metal. The arc-melted alloys were cold pressed under 50 thousand psi and reduced as much as 50 per cent in thickness. A surprising feature of these alloys is that upon annealing in vacuo at 600°C for 24 hours the cold-worked metal became harder rather than softer. This is attributed to the development of a brittle peritectic compound (such as $Al_{11}V$) whose formation was suppressed during the rapid cooling of the arc-melting furnace.

Aluminum will dissolve less than 0.5 per cent vanadium in solid solution, while vanadium will dissolve up to 25 per cent aluminum at room temperature. A maximum solid solubility of 35.3 per cent aluminum in vanadium occurs at 1670°C. Of the four intermediate phases, only σ (Al-V) shows an appreciable solid solubility range (47 to 55 per cent vanadium at 1360°C); this solubility range decreases with decreasing temperature and is almost negligible at room temperature.

*This report is based on a Ph.D. thesis by Donald J. Kenney submitted June, 1953.

Table 1
Summary of Phase Properties

Phase	(Al)	α (Al-V)	β (Al-V)	δ (Al-V)	δ' (Al-V)	(V)
Formula		Al_{11}V	Al_6V	Al_3V	Al_8V_5	
Crystal sym.	F.C.C.	F.C.C.	Hex.	F.C.T.	B.C.C.	B.C.C.
Lattice const. (Å)	$a_0 = 4.0496$ $a_0 = 4.0481^b$	$a_0 = 11.586$	$a_0 = 7.718$ $c_0 = 17.15$	$a_0 = 5.3434$ $c_0 = 8.3257$	$a_0 = 9.207$	$a_0 = 3.031$ $a_0 = 3.069^b$
Space group		$T_h^{11} - \text{FD}3$	$D_{3h}^{14} - \text{O}62c^c$	$D_{4h}^{17} - \text{F}4/\text{mmm}$	$T_d^3 - \text{I}43m$	
Atom/unit cell	4	192	56	16	52	2
Structure ^d	A_1	---^e		D_{022}	D_{82}	A_2
Peritectic temp.	660°C	685°C	735°C	1360°C	1670°C	1825°C ^a

^a Melting point of pure vanadium.

^b Lattice constants of (V) saturated with (Al-V) and (Al) saturated with (Al-V).

^c Highest symmetry group of three possible groups.

^d Strukturbericht designation.

^e No analogous compound reported.

The solid solution phase, (V), is the primary phase to crystallize from the melt in all alloys containing more than 50 per cent vanadium.

The crystal structure of each phase was pursued short of quantitative intensity measurements, and an unambiguous formula is provided for each of the intermediate phases. A correlation of the various phase structures indicates that a marked tendency toward super-lattice formation exists in the aluminum-vanadium system. An aluminum atom exhibits a preference for four nearest vanadium neighbors and four nearest aluminum neighbors arranged tetrahedrally.

II. INTRODUCTION

With the advent of atomic power, which is often conceived as being furnished by a metal furnace burning metal fuel, a major surge of renewed interest has been experienced in physical metallurgy. Although there are many instances where an alloy system has been investigated purely out of academic interest, research on metals and alloys is enhanced by a commercial need for useful materials. Accordingly, the metallurgical literature of the first half of this century is dominated by alloys of such metals as iron, copper and aluminum. However, the index of usefulness for power generating materials must now include nuclear as well as other properties; and so the current literature has been infiltrated with alloys of such laboratory curiosities as zirconium, vanadium, thorium and uranium. Titanium and niobium have also assumed added significance.

The physical and chemical properties of an alloy are hardly predictable from the nature of the pure components. This has necessarily led to the accumulation of large amounts of data in the trial and error search for desirable materials. However from nuclear considerations, it is strictly true that an alloy is no better or worse than the sum of its components since alloying or chemical combination will not effect the nuclear properties of the elements involved. Hence, a list of promising alloys can be quickly compiled from a nuclear viewpoint, and the systems may be then eliminated one by one when experimentation has shown that there is little hope of improving upon the physical and chemical properties of the parent metals.

Phase diagrams are useful in summarizing some of the data collected in the search for new and better alloys and can even

serve as a rough guide for their treatment and behavior. Most of the phase diagrams of the promising binary systems of light metals have been thoroughly investigated with the exception of the aluminum-vanadium system. This is rather surprising in view of the elementary properties of these two metals.

Of all the commercially important metals which entered the atomic era, only aluminum has been extensively employed in the internal structure of atomic reactors. The physical properties of aluminum are well known; but in addition to these, it has a low capture cross section for thermal neutrons (1) and also for fission neutrons (2).

Then, too, vanadium is an excellent structural material for fast reactors (3). Its high melting point, ease of fabrication, and ductility might be sufficient recommendation; but what is more significant, vanadium has an absorption cross-section of about 2.2 millibarns for effective energy neutrons of 1 mev: the lowest cross-section of any metal in the first transition series.¹ The ductility of vanadium is such that the pure metal can be formed into bars, sheets, wires and rods with existing techniques; in addition, it has an elastic modulus-density ratio practically equivalent to that for steel (4). Finally, the abundance of vanadium in the earth's crust is equal to that of copper, zinc and lead combined (5).

Therefore, it would appear highly profitable to investigate the phase relations of the aluminum-vanadium system paying particular attention to those alloys which appear to have some significance for the atomic energy program.

III. REVIEW OF THE LITERATURE

A. Historical Survey

1. Metallography

The literature dealing with the aluminum-vanadium system is meager and contradictory. In order to evaluate the reported

¹Correspondingly, Mg has 0.60 millibarns and Al has 0.40 millibarns. Be is considered to be too brittle for general use, and Al is the last structural metal to have a harmful moderating effect which diminishes with increasing atomic weight. Hence, aluminum and vanadium suggest an alloy of highest tolerable moderating effect and lowest possible cross-section (fast neutrons) of all the light metals.

results, it is necessary to refer to a table of the theoretical compositions of possible intermetallic compounds as shown in Table 2. The system is by no means this complicated, but most of these formulae have a literary existence or an analogue in a similar system and hence will be mentioned occasionally below.

In 1902, Matignon and Monnet (6) studied the grain-refining effect of vanadium upon aluminum-copper alloys; it was mentioned in passing that a residue was isolated by chemical means from an aluminum-vanadium alloy containing 76.9 per cent vanadium. This residue had approximately the composition AlV but the details of this work are not available.

About ten years later, Czako (7) investigated a series of alloys which were prepared by the aluminothermic reduction of vanadium pentoxide. He found that alloys containing less than 10 per cent vanadium (by weight) were malleable. The hardness rapidly increases (20 to 20 per cent vanadium alloys could be pulverized easily) and reaches a maximum at about 53 per cent vanadium. With the addition of still more vanadium, the alloys become softer and the polished sections become free of the troublesome cavities encountered with the high aluminum alloys.

Czako reported further that an alloy containing 1 per cent by weight of vanadium in aluminum, contained crystals of an intermediate aluminum-vanadium phase, the amount of which increased with increasing vanadium content until the 34.5 per cent vanadium alloy consisted almost entirely of this new phase. By treatment of this last mentioned alloy and also a 30 per cent vanadium alloy with dilute hydrochloric acid, crystals containing 37.9 per cent vanadium were isolated. An alloy of 53 per cent vanadium also proved to be microscopically homogeneous with a second intermediate phase. From an alloy of 58.3 per cent vanadium, small crystals with 64.8 per cent vanadium could be isolated. And finally, the alloy containing 79.3 per cent vanadium was also a single phase which Czako suggested was AlV_2 .

Schirmeister (8) studied the technically important effects of the addition of some twenty metals, including vanadium to commercial aluminum. It was reported that an attempt was made to measure the hardness of these various alloys, but the original article is not available for examination. However, the work of Czako and Schirmeister was incorporated by Corson (9) into the probable phase diagram shown in Figure 1. Then too, Fuss (10) reviewed

the work of Schirmeister and quoted him as saying that the 3 per cent vanadium alloy does not shrink or pipe and that alloys containing more than 3 per cent vanadium swell on freezing. Schirmeister found it quite difficult to alloy aluminum with vanadium; this experience was confirmed by Fuss and also by the present work. In testing the physical properties of his commercial aluminum-vanadium alloys, Schirmeister employed a 2 per cent vanadium sheet which was annealed at 300-350°C; he reported a tensile strength of 17,000 to 18,500 psi with an elongation of 27-28 per cent and a Brinell hardness of 35.

Table 2

Theoretical Phase Composition

Formulae	Wt. Per Cent Vanadium
$Al_{11}V$	14.65
$Al_{17}V$	21.23
$Al_{17}V$	23.94
Al_5V	27.41
Al_4V	32.08
$Al_{13}V$	38.62
$Al_{13}V$	45.55
$Al_{18}V_{4/5}$	54.25
Al_3V_2	55.73
$Al_{17}V_6$	61.72
AlV_6	65.40
AlV_2	79.10

In this supplementary investigation, Fuss (10, p. 152) found that the microstructures of aluminum-vanadium alloys were similar to aluminum-iron, aluminum-manganese, and aluminum-molybdenum alloys. Vanadium showed no apparent solid solubility in aluminum and a eutectic was found to exist in the system.

The solid solubility limit has been obtained by an unknown worker (11) who measured the conductivity of aluminum containing small amounts of vanadium. An abstract of a research memorandum from the A.F.C. (French Aluminum Company)

shows that vanadium lowers the conductivity of aluminum, the effect being proportional to the amount of vanadium up to 0.65 per cent vanadium by weight which is the solid solubility limit. Unfortunately, no heat-treatment data are available.

Roth (12) made a thorough study of the solid solubility of vanadium in aluminum by employing lattice constant measurements and conductivity data (Figures 2 and 3). He found the solubility limit to be 0.37 weight per cent vanadium at 630°C, and this value remained unchanged at 500, 350, and 200°C. His alloys were prepared by melting pure aluminum and a 2.5 per cent master alloy in graphite; the alloys thus prepared contained as impurities a maximum of 0.006 per cent iron and 0.005 per cent silicon.

The compound Al_3V was found to have a tetragonal type of crystal structure and the lattice constants were measured by Brauer (13). The alloys were prepared by the reduction of vanadium pentoxide with pure aluminum in cryolyte under argon. The crystals were separated from an alloy containing 10 per cent vanadium by slowly dissolving the alloy in dilute, warm hydrochloric acid. The crystals so obtained analyzed to give 36.5 per cent vanadium.

Mondolfo (14) published no experimental data but did show a micrograph of a commercial aluminum-vanadium master alloy which contained 2.4 per cent vanadium, 0.42 per cent silicon and 0.56 per cent iron. In this picture, he identified five phases as: Al_3V , Al_4V , Al_7V , (Al-Fe-Si), and aluminum solid solution. This would indicate that the low-vanadium portion of the system resembled the aluminum-chromium or aluminum-manganese system, but he did not indicate the extent of his experimental work.

2. Commercial applications

There have been a few commercial applications of aluminum-vanadium alloys. Investigation by Clark (15) into the effect of vanadium in causing resistance to fatigue, increased elongation, and improved homogeneity in the non-ferrous field has shown that 2 per cent vanadium in aluminum materially increases both the hardness and strength of aluminum. A 4 per cent vanadium alloy is strong enough for structural purposes; a 10 per cent vanadium alloy is used to stiffen the framework of airplanes, piston rings, gearboxes, and electrical equipment (16). Alloys containing up to 10 per cent vanadium are malleable, and the binary alloy known as "vanalium" being 3 per cent heavier than aluminum, is

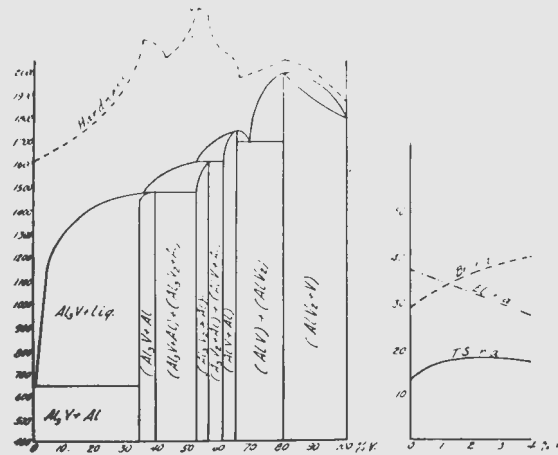


Fig. 1--Probable phase diagram of Al-V system (Corson (8, p. 135)).

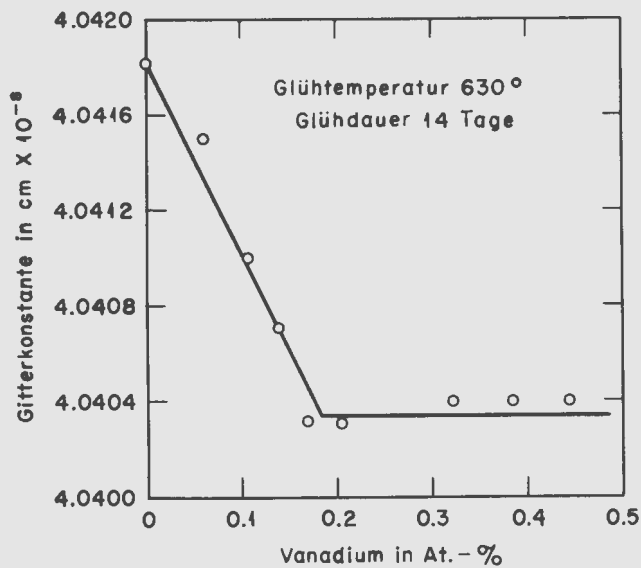


Fig. 2--Lattice constants of aluminum alloys (Roth (11, p. 358)).

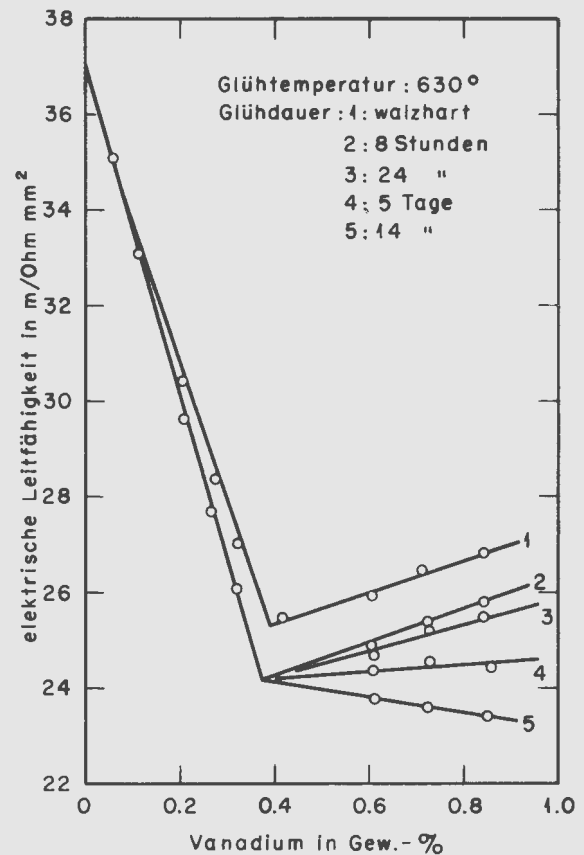


Fig. 3--Conductivity of aluminum alloys (Roth (11, p. 357)).

strong, hard, and corrosion-resistant. Alloys containing about 63 per cent vanadium are hard and very resistant to acids.

In addition to the above-mentioned uses Eborall (17) has shown that vanadium is a powerful grain refiner when added to aluminum in quantities up to 1.5 per cent; vanadium also has a grain-refining effect on aluminum-copper alloys and renders them susceptible to heat treatment (11, p. 472).

B. Discussion of Reported Work

In summary, it might be pointed out that only in the case of the high-aluminum portion of the system has any serious investigation been undertaken, and the results are not conclusive. Czako's (7, p. 141) original work showed a micrograph of an alloy containing 1 per cent vanadium in which white crystals were scattered uniformly throughout a grey matrix. The white crystals, which he identified as Al_3V , made up about 15 per cent of the area. This means that either the picture was not representative of the alloy, or else the white crystals contained far less vanadium than Al_3V . The reason being, of course, that the white crystals cannot contain more than the total amount of vanadium in the sample.

The same criticism can be raised about Roth's (12, p. 357) micrographs of the alloys used to determine what he assumed to be the solubility limit of Al_3V in aluminum. It is interesting to note that if Roth annealed his alloys at 630°C for 14 days, then according to Mondolfo (14, p. 48), his microstructure should have shown crystals of Al_7V surrounded by a matrix of aluminum solid-solution. Then, too, Brauer (13, p. 208) obviously had no knowledge of Mondolfo's work for he slowly cooled a 10 per cent vanadium alloy from 1200°C in order to obtain single crystals of Al_3V .

Perhaps it is pertinent to say that the existence of Al_3V is fairly well established; the existence of Al_7V and Al_4V has been pointedly ignored by all investigators save Mondolfo, who published no data and worked with alloys containing relatively large amounts of iron and silicon; and the existence of any further compounds is uncertain.

C. Summary of Pertinent Facts

For easy reference the pertinent information compiled from the literature survey is presented in tabular form:

Melting Points

Al	660.2°C	
Al ₇ V	750	
Al ₄ V	950	
V	1725	(1935)
V	1780	(1949)
V	1899	(1951)

Density

Al	2.6978 (25°C)	(1938)
Al	2.695 (X-ray, 25°C)	(1935)
Al ₃ V	3.68	
V	5.96	

Crystallography

Al - F.C.C.; \underline{a}_0	=	4.0414 Å.
V - B.C.C.; \underline{a}_0	=	3.0338 Å.
Al ₃ V - F.C.T.; \underline{a}_0	=	5.344 Å; \underline{c}_0 = 8.305 Å.

IV. SOURCE OF MATERIALS

A. Aluminum

Because it contains a large amount of iron and silicon, ordinary commercial aluminum is not suitable as a starting material for equilibrium studies. Since 1925, when electrolytically refined aluminum became available (18), many anomalies appearing in literature of binary aluminum alloys can be credited to the fact that some investigators were using aluminum of extremely high purity while others were not. Hence, a standard has been laid down (19) whereby the minimum purity for aluminum used in equilibrium studies shall be 99.99 per cent, and the other metals used for the work shall be the purest obtainable.

Unfortunately, this high purity aluminum was not available in sufficient quantity for the present work and the following plan had to be adopted: Five pounds of massive aluminum, containing a minimum of 99.75 per cent aluminum, was obtained from the Aluminum Company of America. This metal was used in the practice preparation of alloys, in diffusion samples, and in other studies not critically

dependent upon purity. One pound of massive aluminum, containing a minimum of 99.9 per cent aluminum was obtained from the A. J. Mackay Company. This metal was used in the preparation of all samples whose physical and chemical properties are reported below.

B. Vanadium

It was not possible to procure any large quantity of pure commercial vanadium. However, one pound of 99.5 per cent vanadium was obtained from the Electro-Metallurgical Division of Union Carbide and Carbon Corporation with an assay as follows:

V - 99.5%	O - 0.036%	H - 0.0014%
N - 0.095%	C - 0.19%	All Others - 0.10%

Since vanadium reduced in this laboratory was found to be superior in certain respects to this commercial metal, the latter was only employed in a preliminary survey of the system and in diffusion studies.

The Ames vanadium, which was used in the preparation of the final series of alloys, was prepared by the calcium reduction of vanadium pentoxide in a sealed bomb. The method has been standardized and reported by Long (20) and Powers (21). Pure iodine was used as a booster and the sources of the materials are as follows:

Vanadium pentoxide C. P. (Vanadium Corporation of America)
Analysis: SiO₂, 0.01%; Cl, 0.003%; Fe, 0.005%;
Alkalies, trace.

Calcium (Ames redistilled)
Analysis: Fe, 14 ppm; Mn, 13 ppm; N, 100 ppm.

Iodine U.S.P. XIV resublimed (Mallinckrodt).

No quantitative purity of the metal thus produced is available, but the metal gave a hardness value of Rockwell-B-67, whereas the commercial vanadium gave Rockwell-B-97 under similar circumstances.

C. Alloys

As was mentioned above, aluminum-vanadium alloys are quite difficult to prepare. Solid vanadium dissolves extremely

slowly in molten aluminum, and aluminum has a tendency to distill out of molten vanadium. Then too above 1000°C, contamination from the crucible and atmosphere becomes a formidable problem for vanadium (22).

It was only logical then, to turn to arc-melting as a possible means of avoiding contamination. In a laboratory arc-melting furnace, a d.c. arc is usually struck between a tungsten electrode and the sample, which is resting on a water-cooled copper crucible. The sample is melted and cooled quite rapidly, and the entire operation can be performed in a purified helium or argon atmosphere. The product is generally a bright metallic button which has suffered very little contamination from the furnace.

However, in keeping with their seeming incompatibility, aluminum and vanadium still offered great resistance to alloying by arc-melting. The piece of solid vanadium in the puddle of molten aluminum directly beneath the arc would sink down to the bottom of the crucible where it would remain relatively cool. If too much power were applied to the arc, the aluminum would boil away; when the button was turned over and remelted, the vanadium would again sink to the bottom. Naturally, each time the sample was remelted a little more vanadium would dissolve in the aluminum and if this alloying by attrition is continued long enough a homogeneous sample will be produced.

To insure a macroscopically uniform sample, and, at the same time, to prevent the time consumption from being exorbitant, the following procedure was adopted for the preparation of the final series of alloys: The aluminum and vanadium samples, not exceeding a combined weight of ten grams, were arc-melted and flipped four or five times. The resulting alloys, in the composition range of 40 to 80 per cent by weight vanadium, proved to be too brittle to cold work and were employed in the arc-melted combination. The rest of the alloys were cold-pressed after arc-melting with a reduction of from 30 to 60 per cent. In the composition range of 0 to 30 per cent vanadium, where segregation of the vanadium proved to be unusually troublesome, the arc-melting and cold-working operations were repeated. Samples from the entire series of alloys were then cut or broken as needed for heat treatment, and X-ray or microscopic examination. One of the natural disadvantages of melting such small quantities of metal at a time was that the number of tests that could be performed on any particular alloy was limited.

It was found that careful attention to the loss in weight, if any, of the alloy upon arc-melting eliminated the necessity

of chemical analysis in many instances. However, in the composition range 40 to 60 per cent vanadium a rare but reproducible phenomena occurred which made the nominal composition of these alloys uncertain. After being flipped two or three times in the arc furnace, the alloy would approach a certain critical composition and upon cooling it would shatter or even explode with considerable violence. If the explosion occurred after the alloy had solidified (as judged by the shell-like appearance of the fragments, (see Figure 4)), the alloy was considered usable; however, chemical analysis was necessary since it was impossible to recover all the fragments.



Fig. 4--54% vanadium; as arc-melted. X 1.

Table 3 contains a list of the alloys used in this investigation. The chemical analyses may be taken to be precise to $\pm 0.5\%$. The nominal compositions were obtained by weighing the sample before and after melting and ascribing any loss in weight to a loss in aluminum by evaporation during melting. The column marked Δ refers to the discrepancy between nominal composition and chemical analysis,^a and the column of assigned compositions is composed of nominal compositions whenever they were judged to be reliable. In case chemical analysis is used in assigned compositions, one per cent has been arbitrarily added to the experimental value in order to make it agree with the nominal compositions; it is helpful in examining microstructures to have all compositions referred to the same standard.

^aIt may be noted that the differences are all positive with an average value of about 1%. Furthermore, there is no obvious trend in Δ , such as a regular decrease with increasing vanadium content.

Table 3

Alloys Used in This Work

Alloy designation	Nominal composition	Chemical analysis	Δ	Analyst's reference	Arc-melting reference	Assigned composition
DJK-2-82-2	9.1% V	5.4%		MOB-1-175	BLF-1-M193	6% V
		5.4		DJK-3-58		
-82-3	17.3	17.8		MOB-1-175	-M195	19
-82-4	31.2	30.6		-1-175	-M227	32
-82-5	40.4	40.5		-1-175	-M197	42
		41.3		DJK-3-49		
-82-6	50.4	52.5		MOB-1-175	-M226	54
		53.2		DJK-3-54		
DJK-2-82-7	65.9	62.5		MOB-1-175	BLF-1-M192	66
		64.2		DJK-3-55		
		64.8		DK-1-34		
-82-8	81.5	81.3		DJK-3-48	-M190	82
		81.2		DK-1-34		
-82-9	86.2	85.4		DJK-3-47	-M189	86
-82-10	93.4	93.5		-3-45	-M194	94
DJK-2-106-13	21.2				BLF-2-M559	22
-106-16	38.7	37.7		DK-1-34	-M562	39
DJK-4-44-MC	32.7 ^a	32.2	+0.5	LFB-2-17	-M628	32.7
-MC	36.3 ^a	35.6	+0.7	2-17	-M631	36.3
-MC	38.0	37.4		DK-1-30	-M629	38

^aAlloys that did not lose material due to breakage and were weighed before and after melting.

Table 3 (Continued)

Alloy designation	Nominal composition	Chemical analysis	Δ	Analyst's reference	Arc-melting reference	Assigned composition
DJK-4-44-MC	39.4	47.4		DK-1-30	BLF-2-M630	?
-MC	42.7 ^a				-M633	42.7
-MC	52.4	51.4		DK-1-30	-M634	52
-MC	56.2	52.8		1-30	-M646	54
-MC	66.4	46.2		1-30	-M635	?
		51.1		LFB-2-17		
-MC	78.7 ^a	75.9	+2.8	DK-1-30	-M632	78.7
-MC	90.7 ^a				-M627	90.7
DJK-4-47-MA	14.3 ^a	12.6	+1.7	MEF-2-30	BLF-2-M649	14.3
-MA	17.7 ^a				-M654	17.7
-MA	23.8 ^a				-M664	23.8
-MA	27.2 ^a				-M665	27.2
DJK-4-47-MA	43.8	41.9		DK-1-30	BLF-2-M653	43
-MA	57.6	57.1		DK-1-30	-M651	58
-MA	66.8	65.5	+1.3	1-30	-M652	66
-MA	71.6	50.6		1-30	-M644	52
-MA	82.2 ^a	81.5	+0.7	LFB-2-17	-M662	82.2
-MA	86.1 ^a	84.1	+2.0	-2-17	-M657	86.1

^aAlloys that did not lose material due to breakage and were weighed before and after melting.

Table 3 (Continued)

Alloy designation	Nominal Composition	Chemical analysis	Δ	Analyst's reference	Arc-melting reference	Assigned composition
DJK-4-46-MD	0.4 ^a	0.1	+0.3	MEF-2-30	BLF-2-M660	0.4
-MD	1.6 ^a	1.1	+0.5	2-30	-M675	1.6
-MD	3.5 ^a	2.7	+0.8	2-30	-M661	3.5
-MD	6.3 ^a	4.7	+1.6	2-30	-M650	6.3
-MD	10.1 ^a	7.6	+2.5	2-30	-M659	10.1
DJK-4-46-MD	92.5 ^a	91.5		LFB-2-17	BLF-2-M643	92.5
-MD	94.4 ^a				-M658	94.4
-MD	95.3 ^a				-M656	95.3
-MD	98.6 ^a				-M655	98.6

^aAlloys that did not lose material due to breakage and were weighed before and after melting.

V. APPARATUS AND METHODS

A. Obtaining Thermal Data

Since the system covered such a large range of melting temperatures, it was inevitable that several different techniques had to be employed for obtaining thermal data. The use of a resistance furnace, quartz vacuum tube, and chromel-alumel thermocouple provided the most accurate data; but this method was prohibited above 1100°C by the structural limitations of quartz. The next natural change in technique came at 1500°C , at which point platinum-rhodium thermocouples consistently burn out. The final method, and perhaps the most inaccurate, was the use of an optical pyrometer for observing visual signs of melting in this system up to 1900°C . Naturally, overlapping data were obtained by the three methods, and the results are in good agreement if it is remembered that an uncertainty of as much as 25°C sometimes exists in optical-pyrometer data.

A photograph of the equipment designed specifically for the range, 600 to 1100°C , is shown in Figure 5. The heating was done by a 2500 watt electrical resistance furnace which accommodated a 3 inch outside diameter quartz tube. The power for the furnace was supplied by a 220 volt powerstat driven by a Modutrol motor. The system was evacuated by a 60 liter-per-second-capacity, water-cooled, oil diffusion pump and a Welch Duoseal, "1400", mechanical backing pump. It was necessary to place a D.P.I. Phillips vacuum gauge behind a liquid nitrogen cold finger since the presence of aluminum vapor would be harmful to the gauge. The vacuum could always be maintained below 0.02 microns, even during the initial heating period.

The procedure was to suspend a 1 inch outside diameter, graphite bucket from a rubber stopper at the top of the vacuum head. A 1 inch outside diameter thorium crucible containing the alloy and an alumina thermocouple protection tube was placed inside the graphite bucket, and the whole assembly was suspended in a $2\frac{1}{2}$ inch outside diameter refractory cylinder supported from the bottom of the quartz tube. The usual thermocouple and differential thermocouple connections were made in accordance to recommended procedure (19, p. 9). The differential thermocouple made it possible to measure and, at the same time, control the temperature gradient from the sample to the quartz tube; this gave a fairly constant

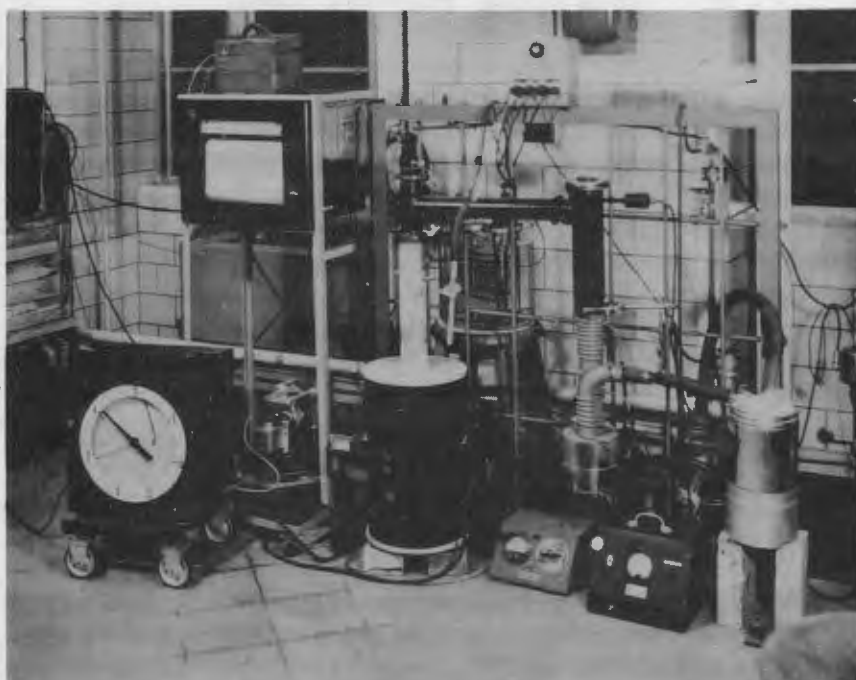


Fig. 5--Thermal analysis furnace.

heating and cooling rate and also served to sharpen and magnify the thermal arrests. This differential thermocouple of chromel-alumel-chromel was connected to a Brown Electronik circular scale potentiometer which in turn energized the Modutrol motor mounted on the powerstat. The thermal emf of the chromel-alumel thermocouple was measured by a Brown Electronik recording strip chart potentiometer of the print-wheel type; this instrument could record both the temperature and temperature gradient in the system. Hence, the thermal arrests could be detected during a constant rate of heating or cooling as described above; or else the powerstat could be fixed at a definite voltage, and the thermal arrests be detected during heating or cooling at constant power in-put.

It was found convenient to maintain the thermocouple cold-junctions at 35°C by means of the constant temperature oil bath shown in Figure 5. The chromel-alumel thermocouple was

calibrated with three melting point standards (Al, Cu-Ag, and Ag) furnished by the National Bureau of Standards; and three or four duplications of each run showed that the thermal arrest of a 10 gram sample could be measured precisely to $\pm 1^{\circ}\text{C}$.

B. Annealing the Alloys

The importance of obtaining equilibrium alloys was accentuated by the four peritectic reactions of this system. Even if the parent alloy contained no segregation on a macroscopic scale, it was safe to assume that no alloy in the range of 10 to 60 per cent vanadium was at microscopic equilibrium in the as-cast or as-arc-melted condition. The removal of segregation or concentration gradients in the parent alloy was described above in the section on alloy preparation; the method for obtaining equilibrium on the microscopic scale will be described here.

Only a small portion (1 to 2 grams) of the cold-worked parent alloy was used in the hope that any remaining concentration gradient would be removed during the annealing run. Ten to fifteen samples were placed in two alundum boats stacked vertically. The samples were vacuum heated in one of several systems typified by the one shown in Figure 6. At the end of the prescribed heating period, these samples were allowed to furnace cool or were quenched in water. Any change in weight upon annealing was measured with an analytical balance; a loss in weight could be attributed to evaporation of aluminum and a gain was assumed to be due to oxidation of the sample. The loss in weight observed never appreciably altered the composition, and if the specimen gained more than 0.3 per cent, it was discarded. Signs of melting or other irregularities were noted before mounting the specimen for microscopic examination.

The vacuum systems employed in annealing experiments (see Figure 6) were composed of a quartz tube within the furnace, a diffusion pump with cold trap and a mechanical fore-pump. The ultimate vacuum attained upon long standing was of the order of 0.001 microns and the pressure was not allowed to exceed 0.02 microns during the heating cycle. A kanthal-wound resistance furnace was regulated by an electronic controller which registered the hot-junction temperature of the chromel-alumel thermocouple inside the quartz tube. Since it was not possible to place the samples in contact with the thermocouple, the annealing temperature may not be relied on to more than $\pm 10^{\circ}\text{C}$. The procedure for quenching was to



Fig. 6--Typical annealing apparatus.

merely relieve the vacuum with argon gas and quickly shake the contents of the quartz tube into a pan of water.

A heating schedule for the alloys used in this work is presented in Table 4. In view of the long periods of time involved, power failures constituted a real menace and samples were sometimes discarded because they were too badly oxidized. The total, accumulated, running time for all the specimens was in excess of 35,000 hours; hence, economy dictated that the fullest possible use be made of each sample. The life history of a typical sample might include an investigation of work hardening, annealing and quench-hardening, melting and macro crystal growth, microstructure, and finally, X-ray patterns in either the solid, powder, or single crystal state.

C. Preparation of Samples for Microscopic Examination

1. Polishing

The specimens for microscopic examination were usually quite small (1 or 2 grams) and were mounted in bakelite plastic.

The grinding was started on a 240 grit sanding disk and was followed in order by numbers 320, 500 and 600 grit papers. The sample was then polished on a soft cloth wheel by using a suspension of Linde A polishing compound in a detergent solution. In the case of alloys containing less than 10 per cent vanadium, the grinding-wheel papers were soaked in benzene-paraffin solution and dried. This procedure prevented an excessive amount of cold work and smearing in the high-aluminum alloy range.

Table 4

Annealing Time for Various Temperatures

Quenching Temperature	Time at Temperature
1100°C	10 hours
1000	50
900	100
800	200
800	24 ^a
750	275
710	325
625 ^b	500
600 ^b	100

a

Furnace-cooled, not quenched.

^bAnnealed 100 hours at 800°C, slowly cooled to 600°C and quenched.

2. Etching

Several different etching procedures were employed, but by far the most versatile was the one which employed immersion in mixed acids. The proportions are: 1000 cc. H₂O, 25 cc. HCl (conc.), 10 cc. HNO₃ (conc.) and 5 cc. HF (48%). The sample was immersed for 10 seconds at 25°C and rinsed with water; if necessary, this etch was repeated and the progress of the successive etchings was observed under the microscope. This etch proved satisfactory in all cases where it was not

necessary to bring out the grain boundaries of the phase, (V), or distinguish between the phases, (Al) and α (Al-V). Phase terminology is discussed below in the section on the microscopic nature of the system.

The best method for bringing out the contrast between (Al) and α (Al-V) consisted in immersing the sample for 10 seconds in a concentrated solution of KOH at 80°C and rinsing with cold water.

Either an electrolytic etching or cathodic etching proved satisfactory for revealing well-defined grain boundaries in the (V) or vanadium solid solution phase. The electrolyte employed in the electrolytic etching was a 3N HNO₃ solution containing 1 per cent by weight of KF; a current density of about 0.1 amps per square cm was found to give good results. The cathodic etching was mainly done as an experiment to test the universality of that method and is described in detail elsewhere (23). The conditions which proved to be the most satisfactory for cathodic etching of aluminum-vanadium alloys were:

Atmosphere -- Argon at 20 microns.
Electrode Spacing -- 15 inches.
Voltage -- 6000 volts.
Current -- 13 milliamps.
Time -- 15 minutes.

A Bausch and Lomb Research Metallograph was used to examine and photograph the specimens. Photomicrographs are presented below in four standard magnifications (75X, 120X, 250X and 500X). It was possible to obtain magnifications up to 1000X but no further information was procured by doing so. Extensive use was made of visual examination of the samples under polarized light. Anisotropic crystals exhibit extinctions in polarized light as the metallographic stage is rotated (24), and two of the four intermediate phases in this alloy system proved to be anisotropic.

D. Preparation of Samples for X-ray Analysis

X-ray diffraction data were used to obtain three types of information: phase identification, precision lattice constants, and crystal structure. Three general methods of X-ray analysis were employed with varying degrees of success to obtain these three different kinds of information. Usually, the powder method gave the best phase identification,

polycrystalline solid specimens gave the most reproducible lattice constants, and when available, single crystals gave information concerning crystal structures.

1. Powder specimens

It was possible to crush alloys in the range 15 to 70 per cent vanadium with a diamond mortar without noticeably broadening the X-ray diffraction lines. It is necessary in studies involving malleable alloys to anneal crushed powder at about 600°C to relieve the strain caused by the cold working. Since this treatment was not necessary in the case of these aluminum-vanadium alloys, the possibility of contamination during annealing was eliminated. This method had the further advantage of giving an X-ray pattern for each observed microstructure. That is, the specimens used for microscopic examination were broken out of their bakelite mountings and given an X-ray analysis without further heat treatment.

The X-ray powder patterns of these alloys at room temperature were obtained on a 11.4 cm diameter Debye-Scherrer camera using filtered copper radiation. The alloy powder was screened through a number 300 mesh and mounted in a thin-wall, glass capillary of approximately 0.04 cm diameter. The back-reflection region of the powder pattern was usually taken concurrently with the Debye picture and was used to calculate precision lattice constants. A symmetrical self-focusing camera of 12.0 cm diameter was employed, and the calculations were refined by the analytical extrapolation first proposed by Cohen (25).

In general, visual examination of the Debye pattern of a two-phase alloy was sufficient to identify the phases present and also estimate their relative amounts. Lattice constant measurements were usually hampered however, because of the frequent superposition of lines from different phases and the consequent difficulty in indexing these lines.

2. Solid samples

Since alloys at the extremities of the system were too soft and too reactive to be used as powdered samples, it was profitable to examine their X-ray spectra in the massive state. The Phillips X-ray spectrometer embodies essentially the same principle as that employed in the original Bragg experiments; a Geiger counter measures the intensity of the beam diffracted from the surface of a solid sample for any given value of the Bragg angle, θ . The bakelite mounted samples used for microstructure determination could be placed

directly in the X-ray unit and a complete phase identification made in the course of an hour. However, this method was limited by the fact that the relative intensities of the different reflections were inherently erratic, and no estimate of the relative amounts of the different phases could be made. This situation became quite critical in the high-vanadium portion of the system where the grain size of the (V) phase was large and the body-centered cubic vanadium structure gave only a few reflections.

The effect of grain size upon the intensities of the reflection measured by the Geiger counter was studied extensively since it was desired to measure the change in lattice constant with composition of the (V) phase. There are only two intensity peaks in the whole back-reflection region of this body-centered cubic phase (copper radiation), and both of these reflections had to be sharply resolved to obtain a precise lattice constant. A schematic drawing of the Phillips X-ray spectrometer is shown in Figure 7. The unit is essentially the same as an asymmetrical, self-focusing camera in that the source, the sample, and the Geiger counter or film all lie on the circumference of the focusing circle. It can be seen that a sample of finite length should be curved and not planar to lie truly on the focusing circle. In the front reflection region where 2θ is small and the focusing circle is large, the plane surface of the sample closely approximates a segment of the circumference of the circle. However, in the back-reflection region where 2θ is large and the focusing circle is small, only a small area of the sample approximates the circumference of the focusing circle; hence, for a large grain sample only a few grains are located in the optimum focusing position.^a

A special sample holder was designed to measure the lattice constant of the (V) phase (Figure 8). The purpose of this instrument was to affect a translation of the sample in a tangential direction to the focusing circle at constant θ . This was done by means of a simple system of gears and racks so that the sample could be remotely controlled while being exposed to the X-ray beam. The procedure was to fix the sample at an approximate value of 2θ , translate the sample to obtain a maximum peak intensity, and then measure 2θ precisely. It was found that in the critical region of 2θ equal to 140° a translation of only 1 mm would make the difference between a large intensity peak and no peak at all. Satisfactory lattice constants were obtained for the vanadium

^aThe focusing circle shown in Figure 7 is really the cross section of a focusing cylinder whose height for this unit is about 1 cm.

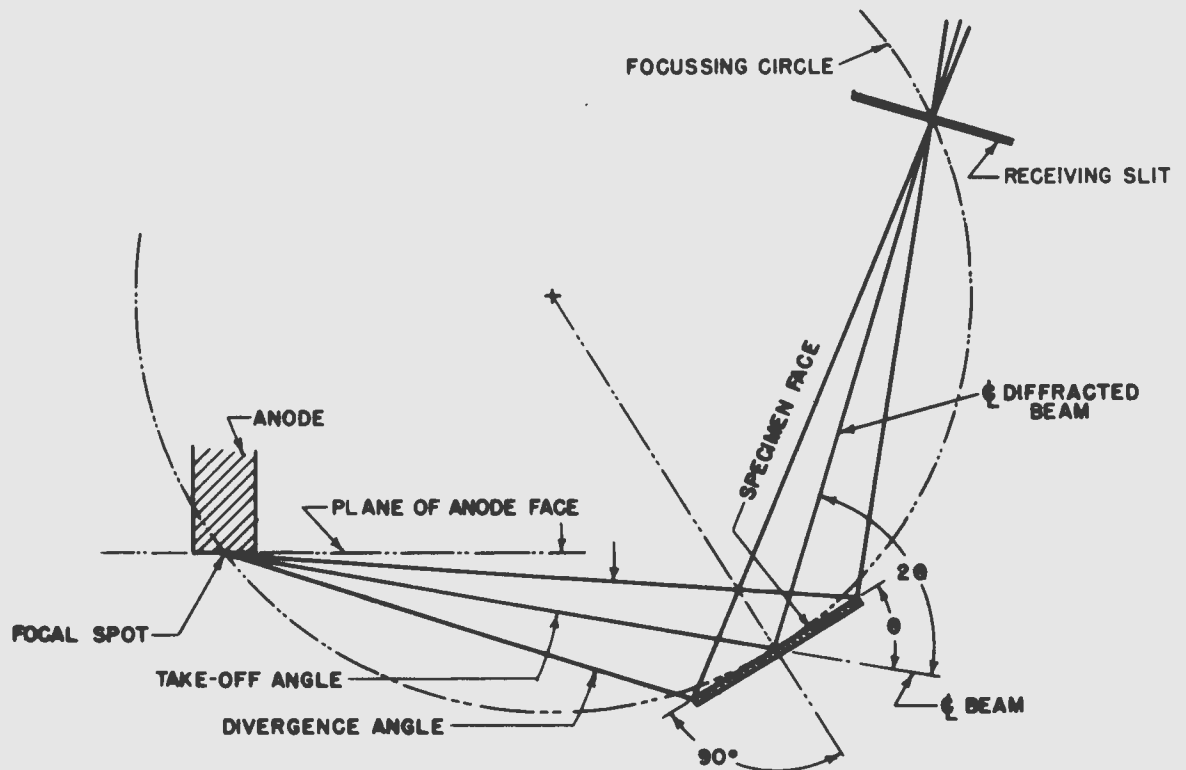


Fig. 7--Phillips X-ray spectrometer (schematic).

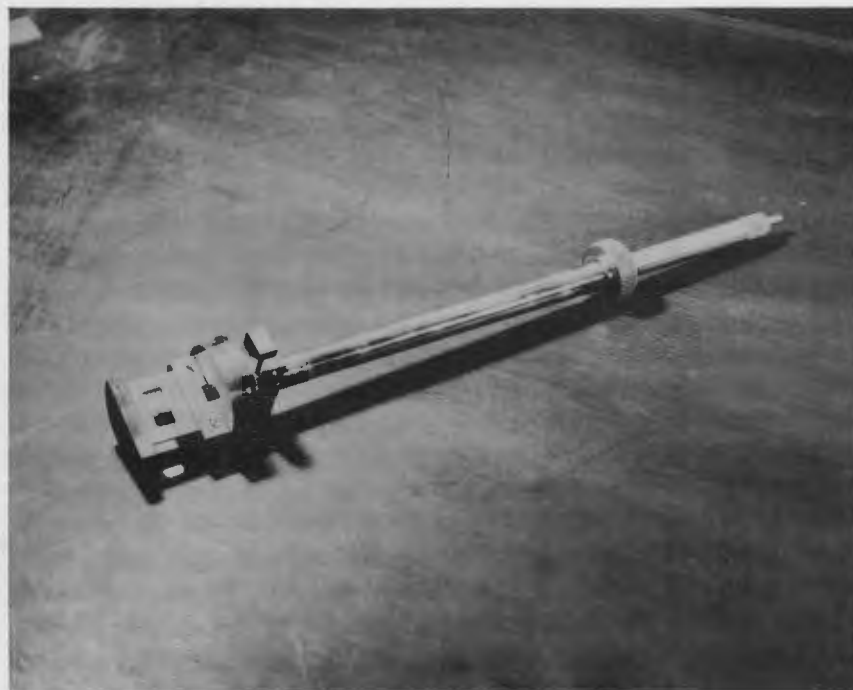


Fig. 8--Solid sample holder for x-ray spectrometer.

solid solution phase by using the graphical extrapolation proposed by Nelson and Riley (26). These constants are reported in the section on the microscopic nature of the system.

3. Single crystals

Single crystals are, of course, invaluable in determining the atomic arrangement in a phase; also, when the powder pattern of a phase is complex, single crystals are often the only means of indexing the pattern and hence, making phase identification. In this investigation, the fullest possible use was made of this phase identification function of single crystals, while crystal structure information was pursued short of quantitative intensity measurements. Single crystal specimens of α (Al-V), β (Al-V), and γ (Al-V) were available. The powder photograph of an alloy containing the α and β phases is black with lines; that is, the error in determining the position of a line is often of the same order of magnitude as the distance between adjacent lines. It is doubtful if proper phase identification could have been made for α (Al-V) and β (Al-V) without the use of single crystal information.

Single crystal data have been gathered from rotation, oscillation, Weissenberg, and precession pictures and are presented below in the section on phase structure.

E. Chemical Analysis

1. Volumetric

All of the alloys were analyzed for vanadium, and the aluminum was then determined by difference. This procedure is not too profitable in the high-vanadium portion of the system, but measured densities when plotted against nominal compositions gave a straight line in this region. The method for volumetric analysis was based essentially upon that worked out by Willard and Young (27) who showed that it was feasible to use ferroin (ferrous o-phenanthroline sulfate) as an oxidation-reduction indicator for the vanadic acid-vanadyl system, provided the hydrogen ion concentration is sufficiently high. The alloys could be dissolved in hot concentrated nitric acid, and after adding sulfuric acid and fuming the solution, it was possible to completely oxidize the vanadium to vanadic acid with an excess of sodium bismuthate. The solutions were then titrated with standard ferrous sulfate using the above-mentioned ferroin indicator. The reported chemical composition of alloys containing more than 10 per cent vanadium may be taken to be precise to 0.5 per cent.

2. Spectrophotometric

Alloys containing less than 5 per cent vanadium were analyzed by a spectrophotometric method; this determination of vanadium is usually based on the reddish-brown color formed by the pentavalent vanadium and hydrogen peroxide in an acid solution. However, a detailed description of the method used here has been given by Telep and Boltz (28), in which a characteristic absorption peak of the complex is measured in the ultra-violet region. Standard curves were constructed by the analytical section of the Ames Laboratory (29).

VI. EXPERIMENTAL RESULTS

A. Macroscopic Nature of the System

1. Density

The density of a series of arc-melted alloys was measured by observing the apparent loss of weight in water and is shown

in Figure 9. The points have been joined by segments of straight lines in a somewhat arbitrary manner. These straight lines may or may not have a real significance since they merely serve to emphasize the linearity of certain portions of the curve and the deviations from average specific volumes of the elements. The room-temperature phase boundaries for the system are indicated by vertical lines and there seems to be some correlation between discontinuities in slope of the specific-volume curve and these phase boundaries. However, it must be emphasized that these alloys are in the as-arc-melted and not the equilibrium condition. Whenever the malleability of the alloy permitted, the density of the arc-melted button was measured after it had been compressed under 50 thousand psi to about the shape of a silver dollar.

2. Hardness

The addition of aluminum to vanadium seems to have little effect on the hardness of either the as-arc-melted or cold-worked metal. All hardness values observed for alloys containing up to 20 per cent aluminum either in the as-arc-melted or cold-worked condition fell within 10 points of 60 on the Rockwell "A" scale.

On the other hand, the addition of vanadium to aluminum has a profound effect on the hardness of the metal (See Figure 10). The high-aluminum arc-melted alloys were cold-pressed under 50 thousand psi and reduced up to 50 per cent. A surprising feature of these alloys is that upon annealing in vacuo at 600°C for 24 hours, some of the cold-worked samples became harder rather than softer. Perhaps this is due to the presence of the brittle peritectic, $Al_{11}V$, whose formation was suppressed during the rapid cooling of the arc-melting furnace.

3. Ageing

A 0.5 per cent vanadium alloy was cast in graphite under an argon atmosphere and rapidly cooled in a stream of air. The alloy was cut up for two test series of ten samples each; the first series was placed in an oil bath at 50°C and the second in a bath at 100°C. Periodically, a sample was removed from each series and its hardness was measured on an arbitrary Rockwell scale. After about 3 hours at 50°C, the first series show a maximum hardness (Figure 11); while the series at 100°C exhibited a maximum hardness after only 40 minutes. In each case the hardness dropped upon extended treatment.

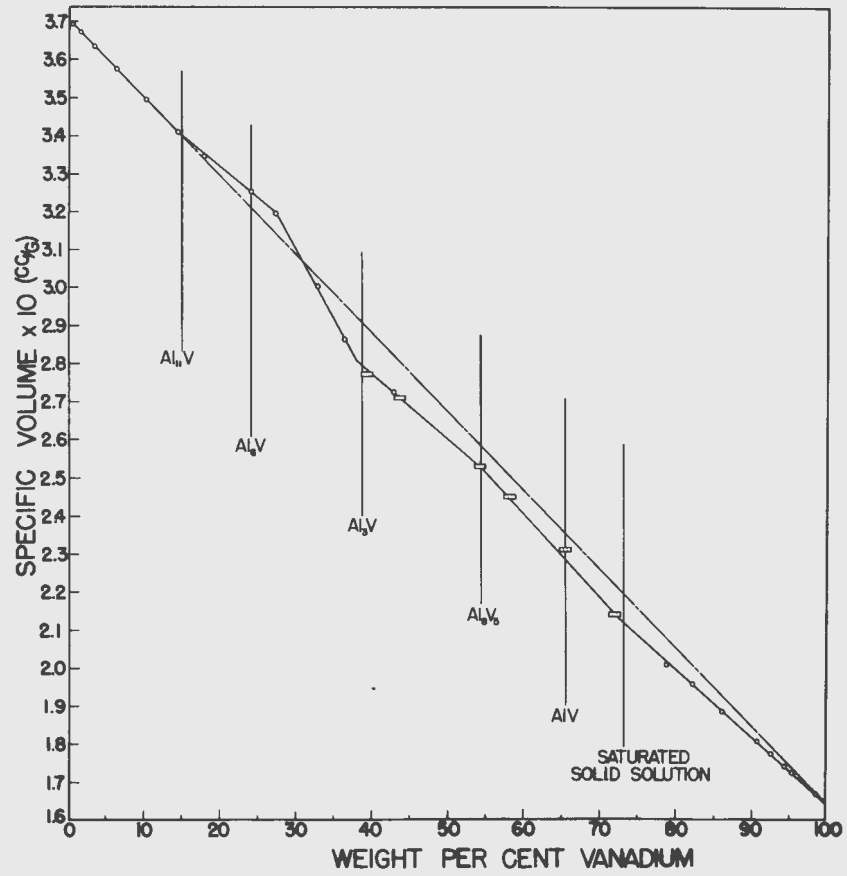


Fig. 9--Specific volume of arc-melted alloys.

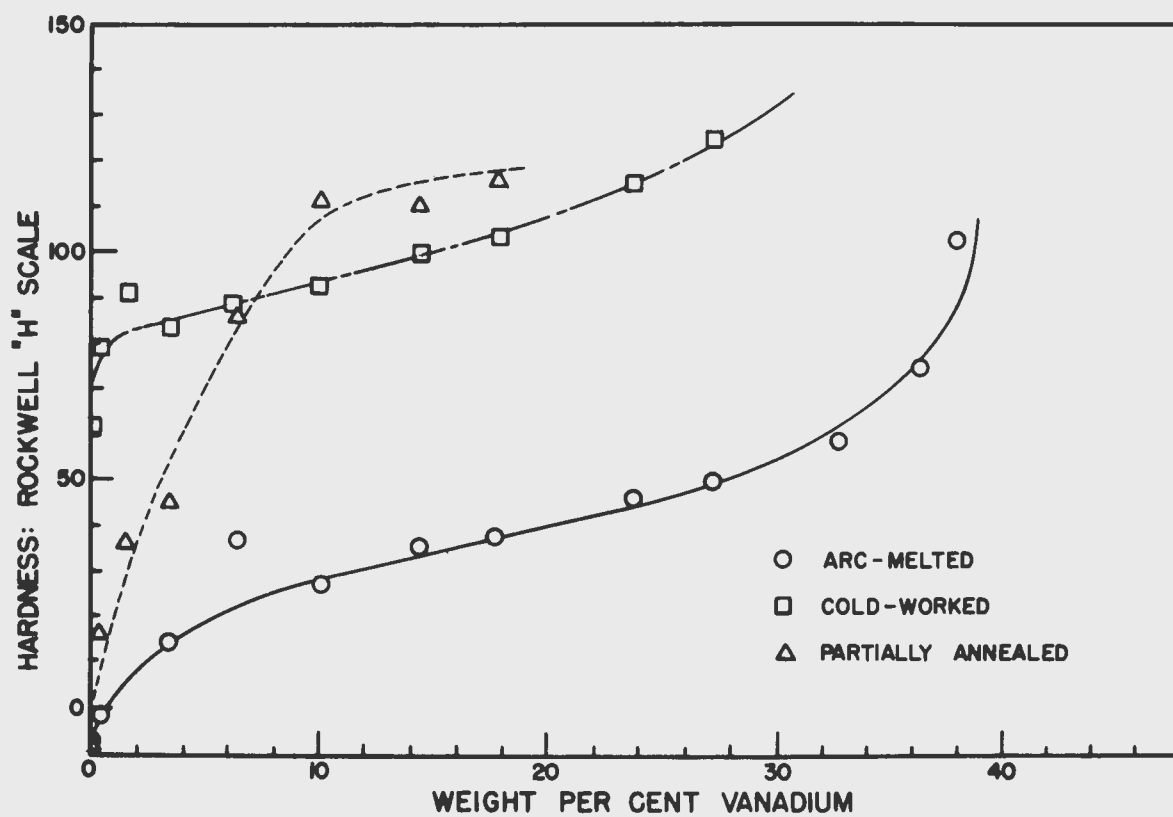


Fig. 10--Hardness of high-aluminum alloys.

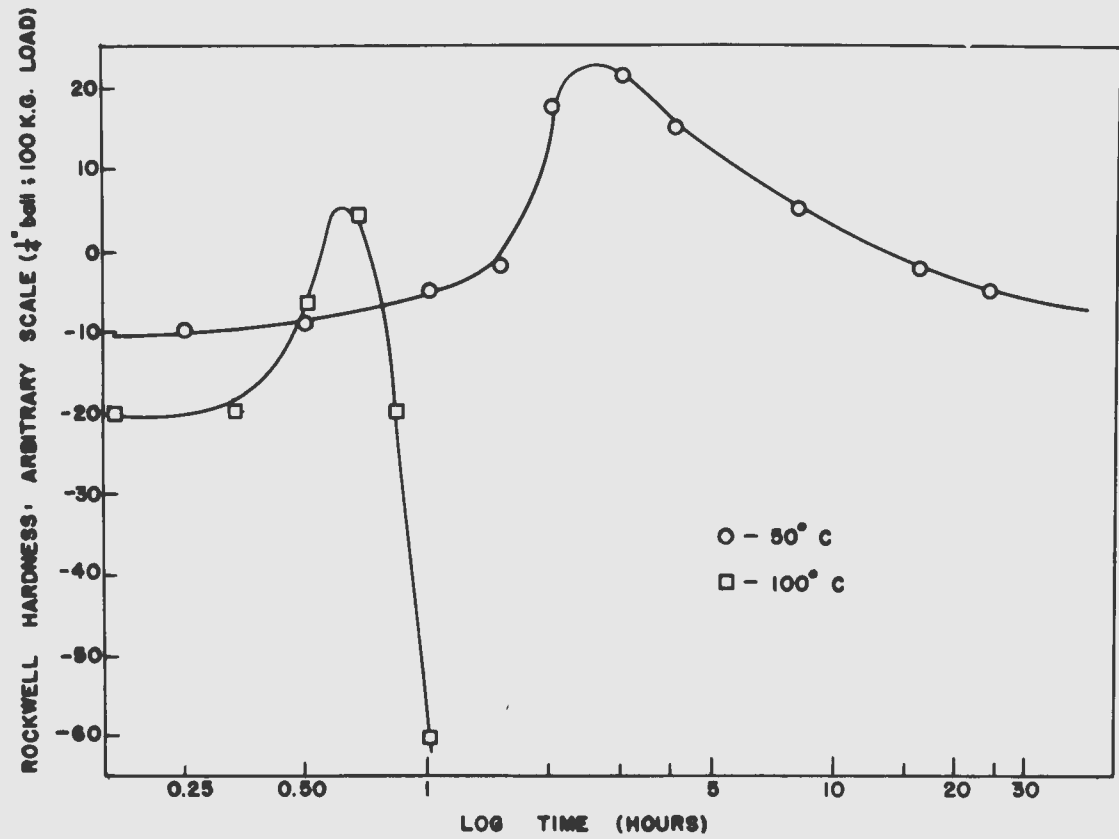


Fig. 11--Age-hardening of an 0.5% vanadium alloy.

Although these samples were not given the rapid quench usually employed to obtain maximum age-hardening (30) they did respond to the subsequent heat-treatment. There appears to be two hardening effects obtained upon the heat-treatment of aluminum-rich alloys. One is perhaps a true age-hardening effect, while the other (occurring in the range of 600°C) is perhaps due to the formation of a hard peritectic compound.

B. Microscopic Nature of the System

1. Introduction

Micrographs and X-ray diffraction patterns have revealed the existence of six phase fields in the aluminum-vanadium system. Phase designation has been made in accordance with the procedure first proposed by Dix and Keith and later modified by Fink and Willey (19, p. 4). The chemical symbols of the elements necessary for the formation of a phase are placed in the order of decreasing atomic percentage and enclosed in parentheses. They are separated by hyphens in order to distinguish them from chemical formulae. If two or more phases would have the same designation according to the above rules, they are distinguished by prefixing Greek letters. It is desirable but not always possible to arrange the Greek letters in alphabetical order, since additional phases may be discovered after the system has already been described in the literature.

In order to facilitate a report of the experimental results, an artifice will be employed whereby the phases are first described as entities unto themselves and later examined in the significance of neighboring phase relationships.

Generally speaking, the agreement between microscopic and X-ray analysis is excellent. However, an uncertainty exists in assigning an exact composition to samples containing between 40 and 70 per cent vanadium. Chemical analysis is meaningless when the sample is not at equilibrium; then too, as mentioned above, explosions would often drastically alter the originally intended composition of an alloy. It was profitable to examine non-equilibrium alloys in the as-arc-melted or partially annealed state since they often revealed a sequence of phase formation.

Therefore each photomicrograph presented below has been assigned a composition (weight per cent vanadium) in accord

with that listed in the last column of Table 3. When it was not possible to determine the composition from chemical analysis or loss in weight, the photomicrograph has been assigned a composition on the basis of the relative amounts of the different phases present. The symbol (E) has been placed after such estimated compositions. Of course, such a procedure presupposes an identification of the phases present and the location of their phase boundaries.

2. Phase properties

(a) (Al). Aluminum will dissolve a small amount of vanadium in solid solution; the solubility limit of 0.37 per cent vanadium at 630°C was determined by Roth (12, p. 357) who employed electrical resistivity and lattice constant measurements. Figures 12 and 13 show the microstructures of (Al) and (Al) with an excess of α (Al-V). The aluminum matrix is usually gouged and pitted in a two phase alloy because of its extreme softness and chemical reactivity. This characteristic is often an aid in identifying the constituents in a microstructure. Very little work was done on this phase since an extremely high purity of aluminum is necessary and as stated above, aluminum of only 99.9% was available. However, it was determined by thermal analysis, that the addition of vanadium neither raises nor lowers the melting point of the (Al) phase, within the limits of experimental errors ($\pm 1^\circ\text{C}$).

(b) α (Al-V). The last intermediate phase to be detected in the aluminum-vanadium system was α (Al-V). This phase does not exist above 685°C and is seldom found in a cast alloy. It is difficult to distinguish this phase from (Al) under the microscope since the two phases have similar etching characteristics. Then too, α (Al-V) and (Al) are both optically inactive under polarized light because both are isotropic. X-ray diffraction patterns of powder samples show the crystal symmetry to be face-centered cubic ($a_0 = 14.586 \text{ \AA}$); this seems to indicate that the crystal may be a super lattice of aluminum which is also face-centered cubic ($a_0 = 4.0496 \text{ \AA}$). α (Al-V) corresponds to the formula Al_{11}V . The extent of solid solubility in this phase is unknown. Typical microstructures of α (Al-V) and (Al) and with β (Al-V) are shown in Figures 14 and 15, respectively.

(c) β (Al-V). Figure 16 shows the single phase microstructure found in a 23.8 per cent vanadium alloy. This phase is probably the one Mondolfo had reference to when he reported Al_7V (14, p. 48). β (Al-V) is usually porous since it can only be formed by a diffusion mechanism and not by a casting operation. Unlike α (Al-V), this phase shows optical activity



Fig. 12--0.4 per cent vanadium. Quenched from 625°C. Aluminum solid solution phase, (Al). Etched with KOH. X250.

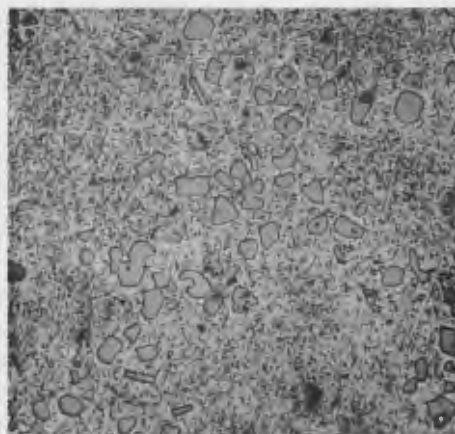


Fig. 13--1.6 per cent vanadium. Quenched from 625°C. (Al) plus small crystals of α . Etched with KOH. X250.

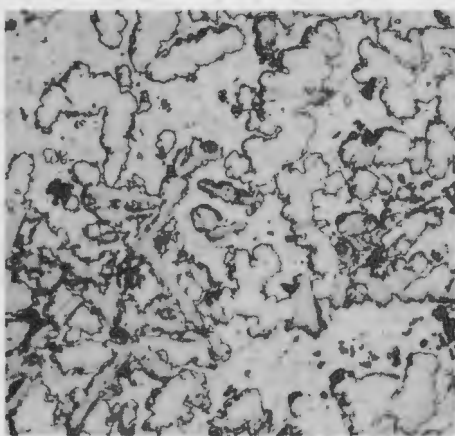


Fig. 14--6.3 per cent vanadium. Quenched from 625°C. Islands of α in (Al). Etched with KOH. X250.

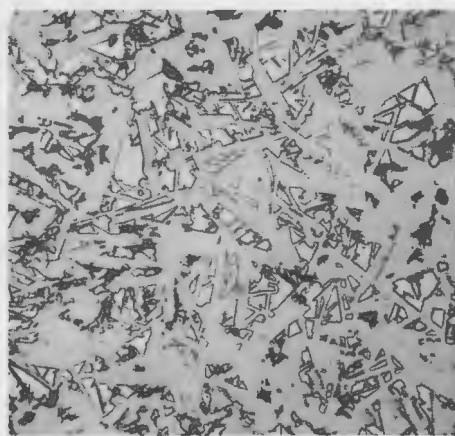


Fig. 15--17 per cent vanadium (E). Quenched from 625°C. Sharp crystals of β in α . Etched with HF-HNO₃-HCl. X250.

under polarized light and hence (Al-V) can be distinguished microscopically from (Al-V). (Al-V) does not exist above 735°C (its incongruent melting point) and corresponds to the formula Al_6V ; it crystallized in a hexagonal unit cell ($a_0 = 7.7184 \text{ \AA}$; $c_0 = 17.15 \text{ \AA}$).

(d) $\gamma(\text{Al-V})$. This phase corresponds to the formula Al_3V and its crystal structure has already been reported by Brauer (13, p. 208). It exhibits an incongruent melting point (peritectic reaction) at 1360°C in much the same manner as its isomorph Al_3Ti (31). $\gamma(\text{Al-V})$ has a much greater optical activity than $\beta(\text{Al-V})$ and hence can be immediately identified under polarized light; a typical micrograph of Al_3V is shown in Figure 17. Table 5 shows that the lattice constants of $\gamma(\text{Al-V})$ in a two-phase region depend upon the other phase present; this is the classical illustration of a solubility range in an intermediate phase. The change in the ratio of c_0 and a_0 across the one-phase region probably represents a solubility range of about 1 per cent, but no quantitative calculations can be made. However, the constants in the β plus γ and γ plus δ regions show no measurable dependence upon temperature which suggests that the phase boundaries are essentially vertical. The lattice-constant measurements were made on powdered specimens using a 12 cm diameter back-reflection camera.

(e) $\delta(\text{Al-V})$. In the copper-zinc system, the intermediate phase designated as γ -brass crystallizes in a body-centered cubic structure with 52 atoms per unit cell (32). $\delta(\text{Al-V})$ is isomorphous with γ -brass and corresponds to the formula Al_8V_5 ; the diffraction lines on a powder diagram of $\delta(\text{Al-V})$ show no splitting due to rhombic distortion as in the case of Al_8Cr_5 (33). A typical micrograph of $\delta(\text{Al-V})$ is shown in Figure 18; this phase shows no optical activity under polarized light and can therefore be easily distinguished from $\gamma(\text{Al-V})$ (see Figure 19). $\delta(\text{Al-V})$ is stable up to 1670°C (its incongruent melting point by optical pyrometer) and seems to have a considerable solid solubility range at 1360°C.

The data in Table 6 can be interpreted to give a rough description of the solubility range of $\delta(\text{Al-V})$. It must be borne in mind that the addition of an aluminum atom expands the crystal lattice (see Figure 2 and Figure 28), and hence, an increase in lattice constant represents an increase in aluminum content for this cubic phase. The measurements were made with a 12 cm diameter back-reflection camera on powdered specimens which had showed either γ plus δ or δ plus (V) under the microscope. Therefore, it seems that there is little or no solid solubility below 600°C but that the extent of solubility increases with increasing temperature. Furthermore, the saturated solid solutions on either side of the

Table 5
Lattice Constants of γ (Al-V)

Compn.	Quench temp.	a_o^a	c_o/a_o^a	a_o^b	c_o/a_o^b
36.3%V	625°C	5.344 \AA	1.5580		
36.3	710	5.343	1.5582		
36.3	800	5.344	1.5581		
38	800	5.342	1.5589		
38	800	5.342	1.5584		
43	800			5.348 \AA	1.5545
38	900	5.343	1.5584		
42.7	900			5.347	1.5549
42.7	1000			5.345	1.5552
36.3	1100	5.343	1.5582		
38	1100	5.341	1.5587		
38	1100	5.343	1.5582		

^a Constants of γ in the two-phase region, $\beta + \gamma$.

^b Constants of γ in the two-phase region, $\gamma + \delta$.

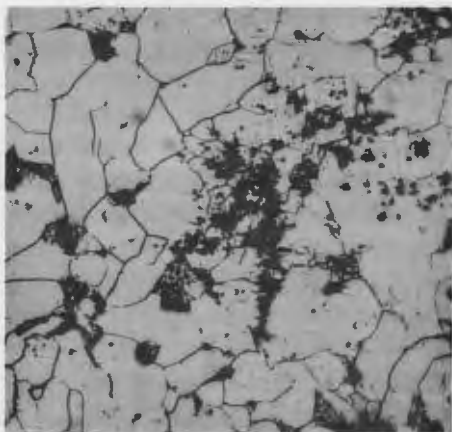


Fig. 16--23.8 per cent vanadium. Quenched from 710°C. One phase, β (Dark areas are voids). Etched with HF-HNO₃-HCl. X250.

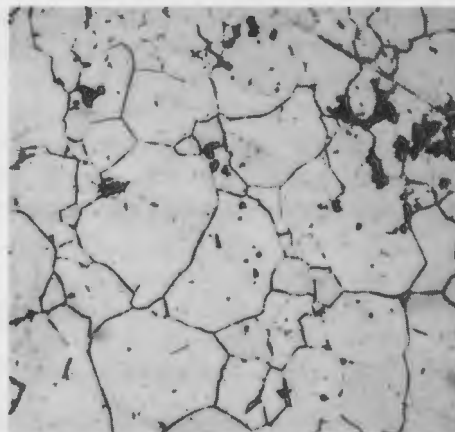


Fig. 17--38 per cent vanadium. Quenched from 800°C. One phase, γ . Etched with HF-HNO₃-HCl. X250.

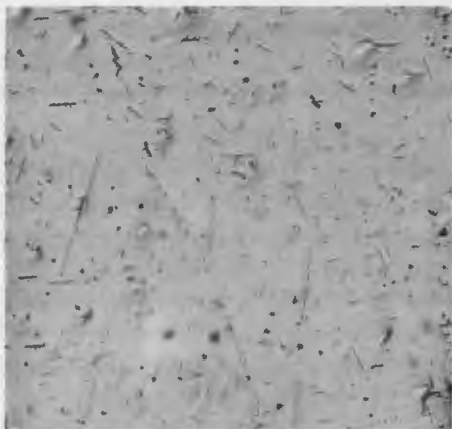


Fig. 18--56 per cent vanadium (E). Quenched from 600°C. Fine needles of (V) in δ . Etched with HF-HNO₃-HCl. X250.

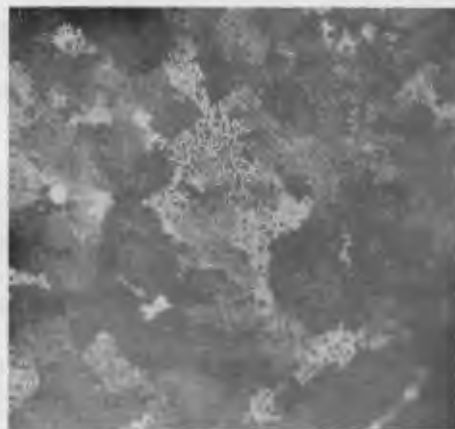


Fig. 19--43 per cent vanadium. Quenched from 800°C. Polarized light. Large grains of γ (alternately bright and dark) containing small grains of δ (always dark). Compare Fig. 55. Etched with HF-HNO₃-HCl. X75.

one phase region increase in aluminum content with increasing temperature.

(f) (V). Vanadium will retain up to 25 per cent by weight of aluminum in solid solution when furnace cooled from high temperatures. Only a rough estimate of the room-temperature saturation can be made, since experience has shown that equilibrium is difficult if not impossible to attain below 600°C.

As might be expected, alloys in this solid solution range were quite similar to pure vanadium. They were characteristically hard and lustrous but easily pitted by etching reagents.

Table 6
Lattice Constant of α (Al-V)

Quench temp.	$a_0(\gamma + \alpha)$	$a_0(\alpha + (V))$
600°C	9.205Å	9.208Å
900		9.223
1000	9.241	9.233
1100	9.248	9.240

The addition of large amounts of aluminum in solid solution improved the appearance of the microstructures, but as yet no highly satisfactory etching procedure has been obtained for pure vanadium or high vanadium alloys. The microstructures show a single phase region extending from pure vanadium over as far as 78.7 per cent vanadium (Figures 20, 21, 22, 23, 24 and 25). It was first thought that 78.7 per cent marked the limit of solid solubility in (V) since higher magnifications at this composition (Figures 26 and 27) revealed the presence of small particles at the grain boundaries. However, this precipitation phenomenon was found to occur in alloys of higher vanadium content (Figure 23). Then too, X-ray measurements placed the solubility limit at 73 per cent vanadium. Therefore, the best interpretation is that these particles are oxide or nitride impurities precipitated along the grain boundaries.

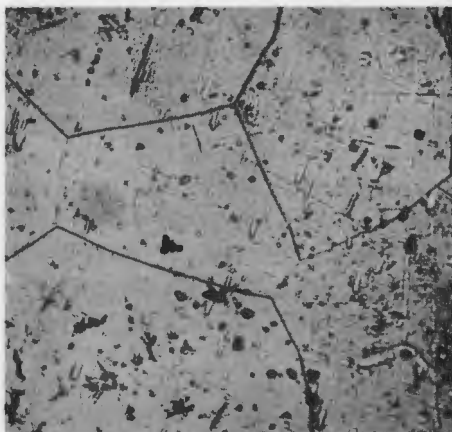


Fig. 20--Vanadium as arc-melted from the bomb reduced metal. Cathodic etch. X120.

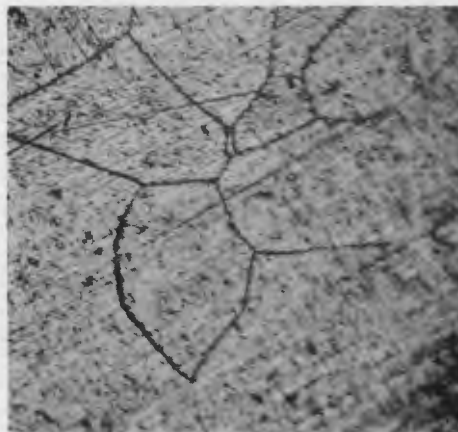


Fig. 21--98.6 per cent vanadium. Quenched from 600°C. One phase, (V). Electrolytic etch. X75.

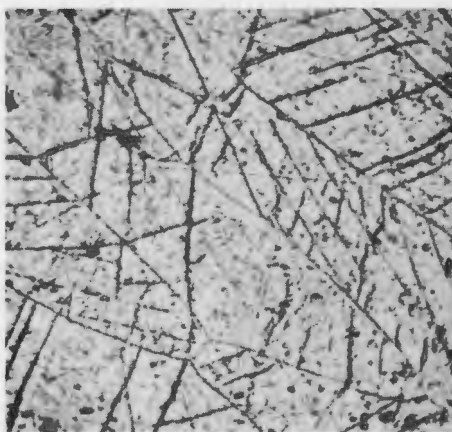


Fig. 22--92.5 per cent vanadium. Quenched from 600°C. One phase, (V). Electrolytic etch. X75.

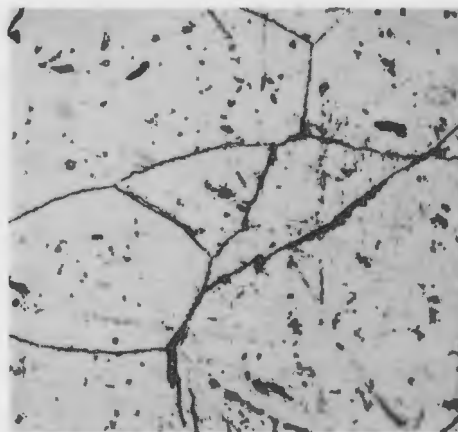


Fig. 23--86.1 per cent vanadium. Quenched from 600°C. One phase, (V). Electrolytic etch. X250.

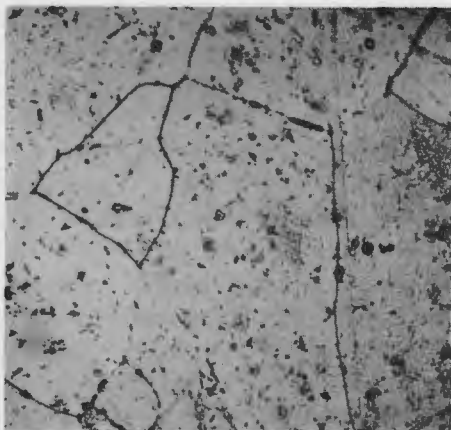


Fig. 24--82 per cent vanadium.
As arc-melted. One phase, (V).
Cathodic etch. X120.

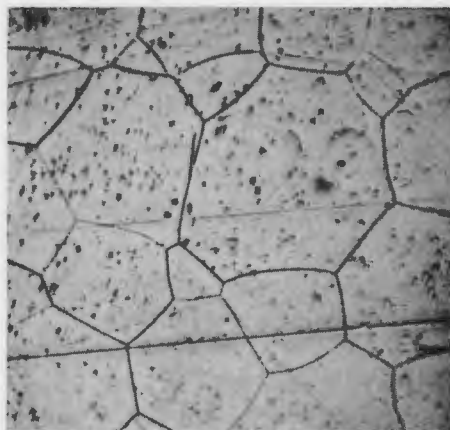


Fig. 25--78.7 per cent vanadium.
Quenched from 900°C. One phase,
(V). Electrolytic etch. X75.

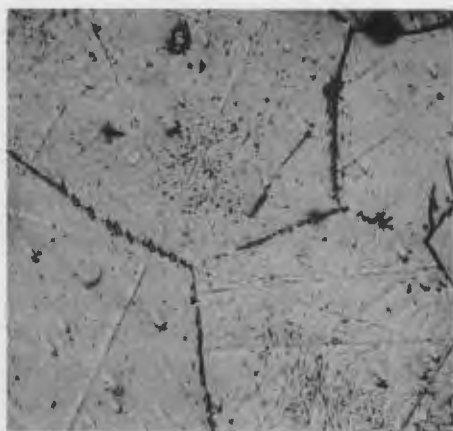


Fig. 26--78.7 per cent vanadium.
Quenched from 900 C. Small oxide
or nitride impurities at the grain
boundaries. Electrolytic etch.
X250.

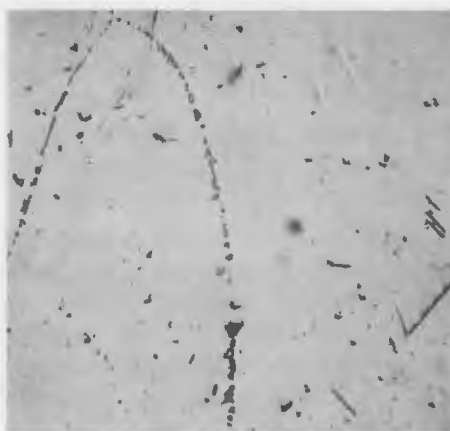


Fig. 27--78.7 per cent vanadium.
Quenched from 1000°C. Oxide or
nitride impurities at the grain
boundaries of (V). Electrolytic
etch. X250.

The X-ray pattern of (V) shows only diffraction lines of pure vanadium, and the lattice constant increases with increasing amounts of aluminum. This means that the solid solution is of the substitutional type in which aluminum atoms take up random positions in the vanadium body-centered cubic lattice.

A precise measurement of the change of lattice constant with composition indicates the extent of solid solubility at various temperatures. Figure 28 shows a plot of lattice constant against atomic per cent vanadium; the lattice constants were taken from measurements made on quenched solid specimens using the X-ray spectrometer. The lattice constant is independent of temperature in a one-phase region and does not change with composition in a two-phase region.

3. Phase relations

The limit of solid solubility for the (V) phase as shown by lattice constant measurements is well substantiated by micrographs. Figures 29 and 30 show the formation of α (Al-V) from (V) by nucleation and grain growth; this mechanism is characteristic of a solid precipitation reaction such as crossing a solvus during cooling. Figures 29 and 30 are interpreted thusly: (V) solidifies completely from the melt forming the large equiax grains which are typical of this solid solution phase. Upon further cooling, the solid solution becomes saturated with α (Al-V). The large amount of precipitation at 600°C (Figure 30) indicates a considerable dependence of solubility upon temperature. When annealed at higher temperatures (Figures 31, 32 and 33), the precipitate becomes more coarse and migrates to the grain boundaries. The whole process may be summarized by the non-equilibrium sample shown in Figure 34; the assumption here is that a concentration gradient is equivalent to a time gradient. That is, if the super-saturated solution could be observed at some temperature such as 900°C, the passage of time would be marked by the coarsening of the precipitate and its migration to the grain boundaries.

In discussing microstructures, it is convenient to refer to a model such as shown in Figure 35. For the sake of the discussion, some of the alloys have been classified into the composition ranges A, B, C, etc.; and hence, the microstructures from Figure 29 and Figure 34 may be described in terms of the hypothetical alloy, A, shown in Figure 35. It must be noted that no matter how drastic the heat treatment, alloys in the range of A all give evidence of having been completely (V) at one time, (See Figure 33).

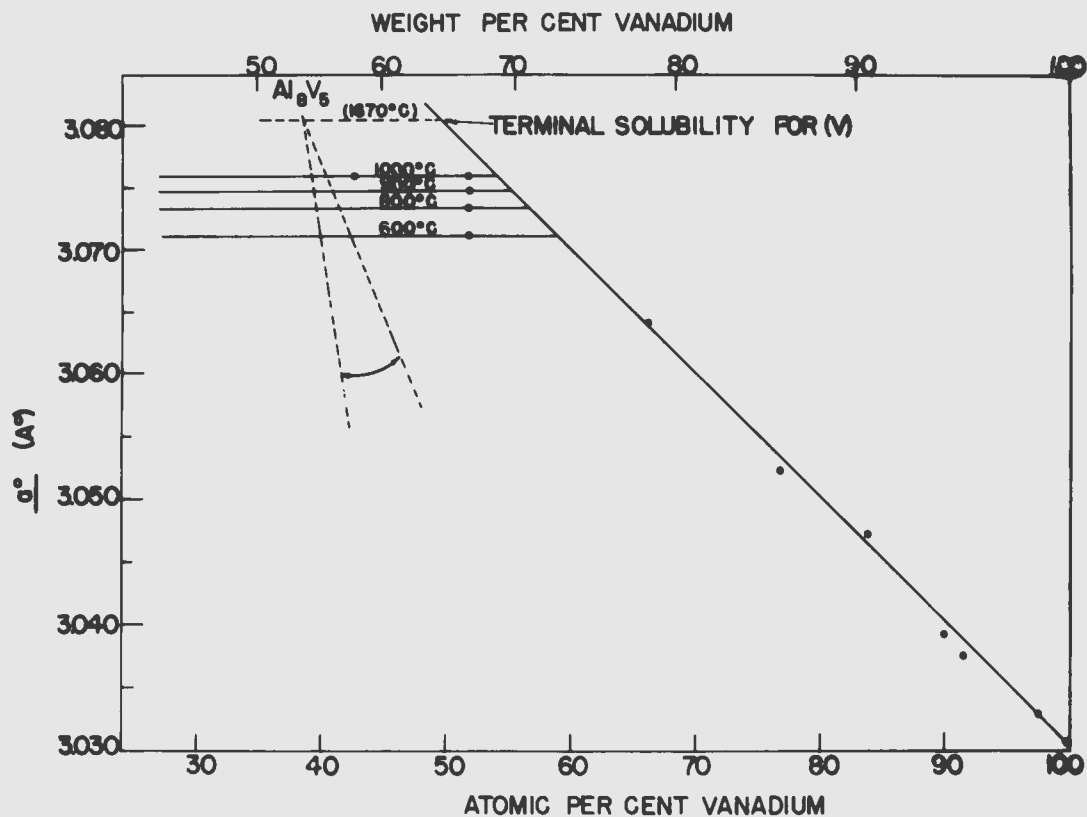


Fig. 28--Lattice constant of (V) as a function of composition.

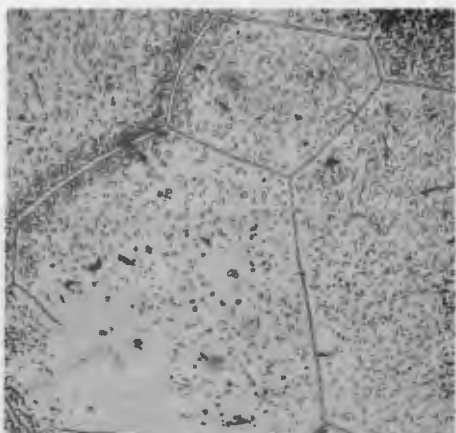


Fig. 29--70 per cent vanadium (E). Furnace cooled from 800°C. Precipitation of δ and migration to the grain boundaries of (V). Etched with HF-HNO₃-HCl. X250.



Fig. 30--66 per cent vanadium. Quenched from 600°C. Heavy precipitation of δ from (V). Etched with HF-HNO₃-HCl. X250.

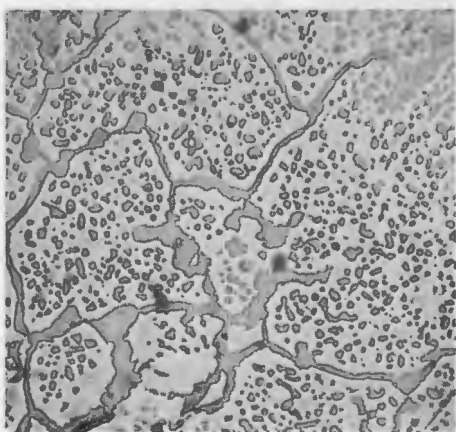


Fig. 31--66 per cent vanadium. Quenched from 900°C. Precipitate in Fig. 30 beginning to agglomerate. Etched with HF-HNO₃-HCl. X250.

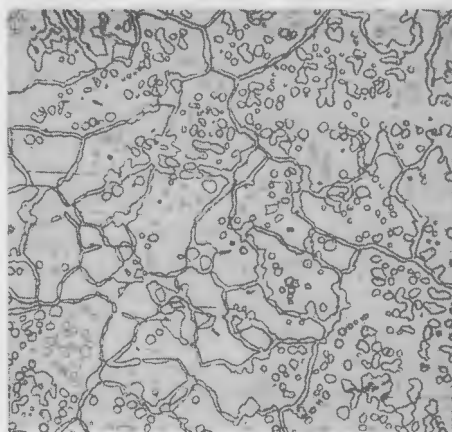


Fig. 32--66 per cent vanadium. Quenched from 1100°C. δ within the grains and at the grain boundaries of (V). Etched with HF-HNO₃-HCl. X75.

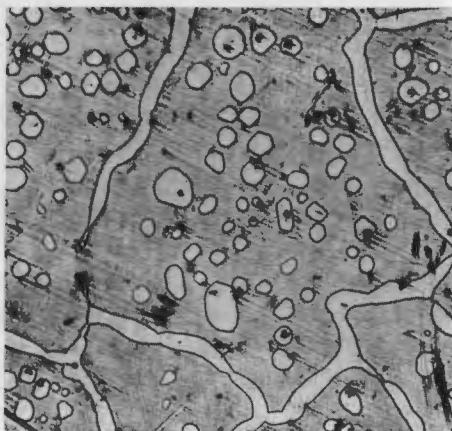


Fig. 33--66 per cent vanadium. Quenched from 1100°C. δ within the grains and at the grain boundaries of (V). Etched with HF-HNO₃-HCl. X250.

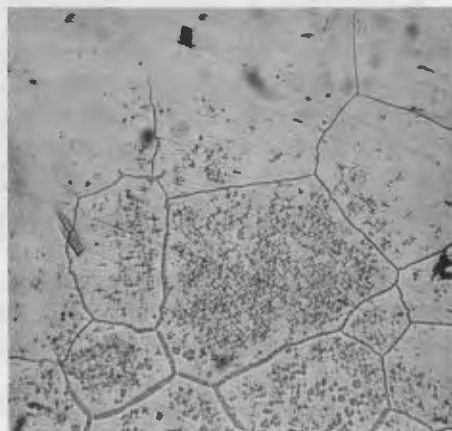


Fig. 34--Concentration gradient. As arc-melted. Etched with HF-HNO₃-HCl. X250.

As more aluminum is added to the alloys, a transition range is approached in which it becomes increasingly clear that the microstructures correspond to the hypothetical alloy B instead of A. In Figures 36, 37 and 38, the remains of the large equiax grains are no longer evident. (Compare Figure 31 with 38, and also 33 with 37.) The alloy B (Figure 35) represents this situation in which the melt can no longer solidify completely before δ (Al-V) begins to form. Because of the noticeable difference in grain size between Figure 30 and 36, an estimation based on the microstructures may be made to place the terminal solid solubility point at 65 per cent vanadium. That is, the original grains of (V) in Figure 36 were coated with peritectic reaction rim before they had a chance to grow large as they did in Figure 30.

Significantly, there is no place where δ (Al-V) is primary to (V) (Figures 39, 40, 41 and 42); this is exemplified by Figure 41 in which the fish-spine crystals of (V) are typical of primary dendrites--that is, the first phase to solidify from the melt. Solid precipitation particles can still be seen in the dendrites of Figures 39 and 40, but they have been annealed away in Figure 42. With still higher concentrations of aluminum, a one phase alloy is approached at about 55 per cent vanadium as shown in Figure 18.

Alloys in the composition range of C (Figure 35) show a radical change from previous microstructures. Figure 43 is interpreted as a non-equilibrium, three phase alloy of this composition range in which the primary dendrites of (V) are surrounded by δ (Al-V) which in turn is surrounded by finely divided σ (Al-V) precipitated after the alloy had completely solidified. The finely divided σ phase etches much more rapidly than the other phases and will often appear completely black in such a three phase alloy.

The addition of more aluminum will give a micrograph of the type shown in Figure 44; σ (Al-V) begins to form before the melt can solidify completely. The cooling history of samples in the range of C is best explained in terms of the classical peritectic reaction which usually leaves the system in a state of meta-stable equilibrium. As the alloy approaches the first temperature horizontal, and primary dendrites of (V) become coated with δ (Al-V); the reaction being



The reaction proceeds at a slow rate because it involves a solid diffusion process, and the alloy supercools. That is, the heat evolved is not sufficient to arrest cooling long

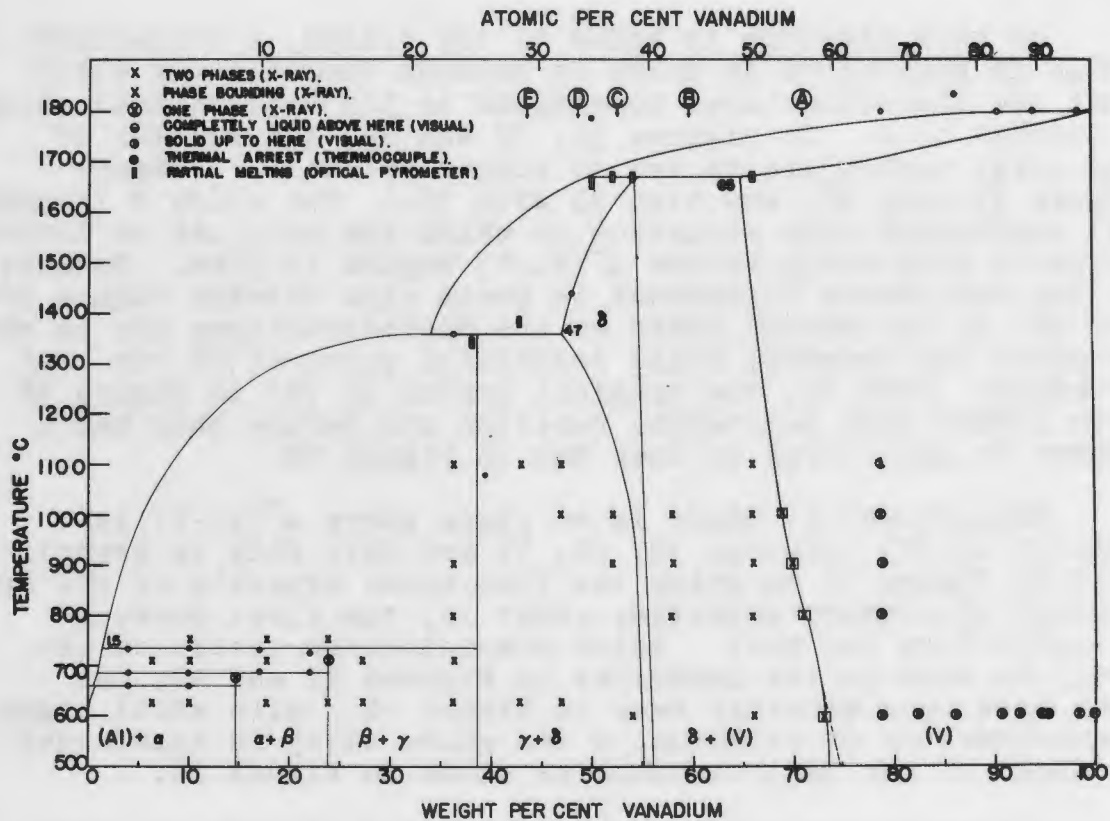


Fig. 35--Thermal and X-ray data for the aluminum-vanadium system.

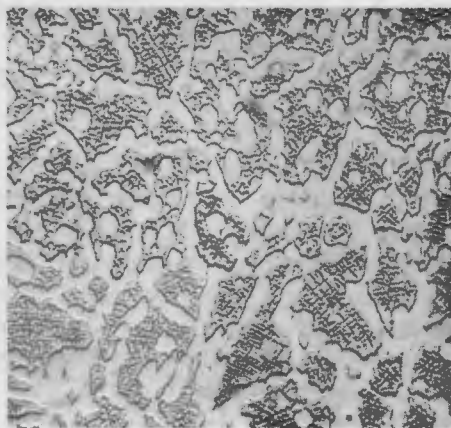


Fig. 36--64 per cent vanadium (E). Furnace cooled from 800°C. Contour lighting. δ in relief from (V) matrix. Etched with HF-HNO₃-HCl. X250.

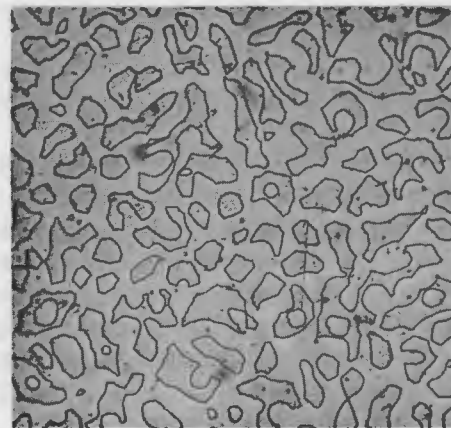


Fig. 37--62 per cent vanadium (E). Quenched from 1100°C. δ (continuous) plus (V). Etched with HF-HNO₃-HCl. X250.

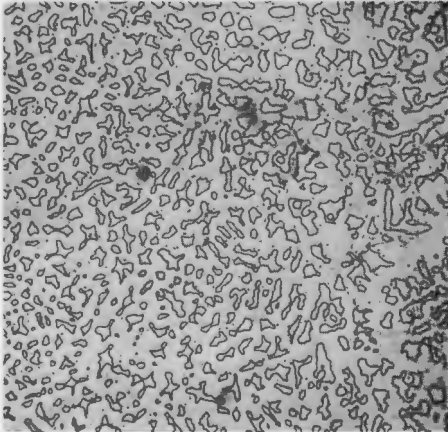


Fig. 38--62 per cent vanadium, (E). Quenched from 900°C. (V) in a matrix of δ . Etched with HF-HNO₃-HCl. X250.

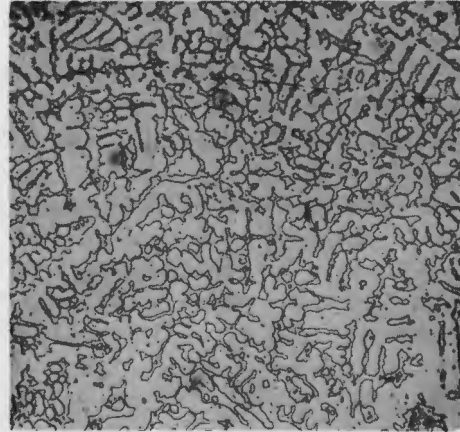


Fig 39--60 per cent vanadium (E). Furnace cooled from 800°C. Dendrites of (V) in the δ matrix. Etched with HF-HNO₃-HCl. X250.

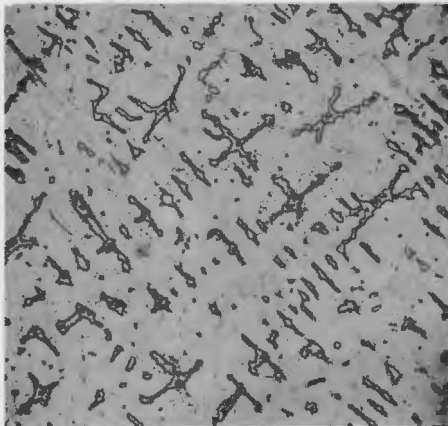


Fig. 40--58 per cent vanadium. Quenched from 600°C. Dendrites of (V) in δ . Etched with HF-HNO₃-HCl. X250.

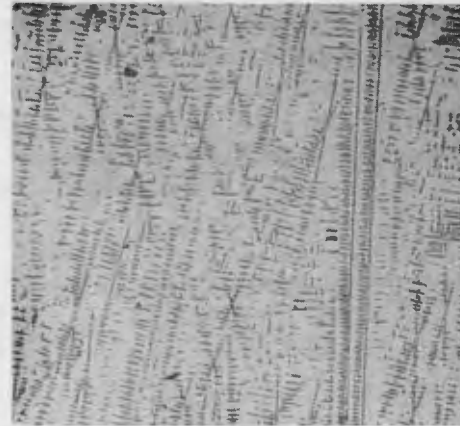
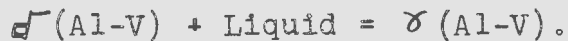


Fig. 41--58 per cent vanadium. Quenched from 800°C. Dendrites of (V) in δ . Etched with HF-HNO₃-HCl. X75.

enough for all the (V) to react with the melt. When the next temperature horizontal at 1360°C is reached,^a σ (Al-V) becomes coated with δ (Al-V); the reaction being



Hence, at the moment the alloy becomes completely solidified, it contains concentric layers of (V) surrounded by σ (Al-V) surrounded by δ (Al-V). Naturally, a large concentration gradient exists across the σ (Al-V) layer, and upon further cooling, part of this layer becomes supersaturated with δ (Al-V) which precipitates out of the solid solution. Upon low-temperature annealing, it is possible to eliminate the (V) dendrites (Figure 45) and even eradicate the concentration gradient entirely at higher temperatures (Figures 46 and 47).

As more aluminum is added to the system, it becomes evident that (V) can no longer be formed and σ (Al-V) is now the first to crystallize from the melt. (See Figure 35, composition range D.) That σ is the primary phase in Figure 48 can be shown by the residual outline of large equiax grains of σ which is absent in Figures 46 and 47. The addition of still more aluminum indicates that σ (Al-V) is able to retain a large amount of δ (Al-V) in solid solution at high temperatures (Figures 49 and 50); at lower magnifications the grains appear black with finely divided precipitate.

A microstructure transition, analogous to the one shown by Figures 30 and 36, occur on increasing the aluminum content from the range D to E. There is a noticeable difference in grain size between Figures 49 and 52. This difference has been taken to indicate that the terminal solid solubility point lies approximately at 47 per cent vanadium (see Figure 51). The sharp distinction between δ (Al-V) at the grain boundaries and δ (Al-V) within the grains of Figure 51 is probably due to the formation of δ first by a peritectic reaction and latter by precipitation in the solid state. Upon annealing, the material at the grain boundaries will then agglomerate the finely divided precipitate in its immediate vicinity.

The significance of the series shown in Figures 53, 54, 55 and 56 is that in no instance does δ (Al-V) appear as primary dendrites in equilibrium with σ (Al-V). Therefore, since (V) is always primary to σ and σ is always primary to δ ,

^aThe peritectic reaction has the effect of removing vanadium from the system and shifting the composition to the left in Figure 35.

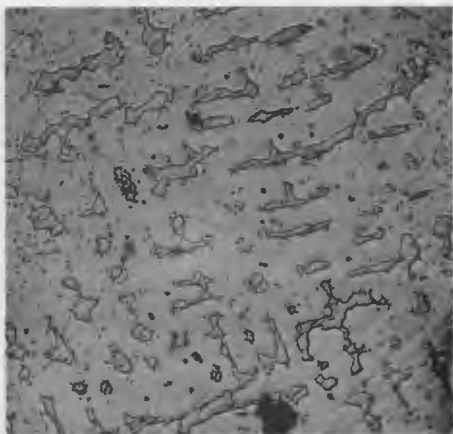


Fig. 42--58 per cent vanadium. Quenched from 1000°C. Dendrites of (V) in δ . Etched with HF-HNO₃-HCl. X250.



Fig. 43--54 per cent vanadium. As arc-melted. Light dendrites of (V) in grey δ . Finely divided γ . Etched with HF-HNO₃-HCl. X250.

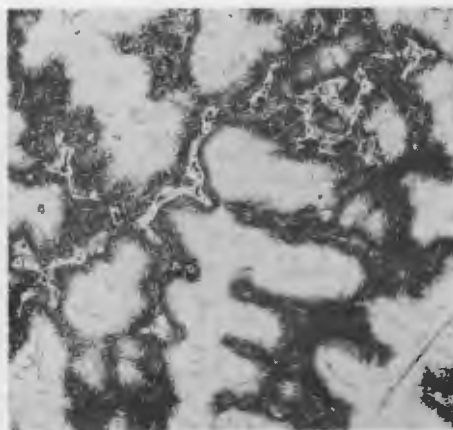


Fig. 44--52 per cent vanadium. Quenched from 625°C. Dendrites of (V) in δ . Long crystals of γ in finely divided γ . Etched with HF-HNO₃-HCl. X250.

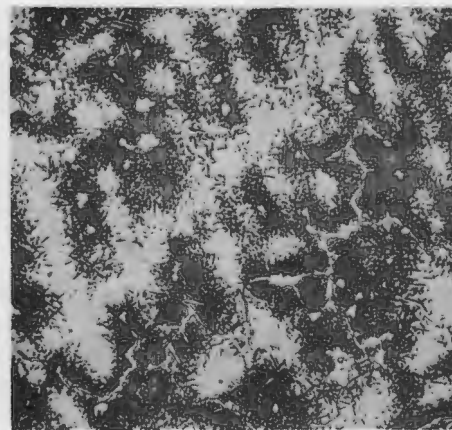


Fig. 45--52 per cent vanadium. Quenched from 800°C. Same as Fig. 44 except (V) has disappeared. Etched with HF-HNO₃-HCl. X250.

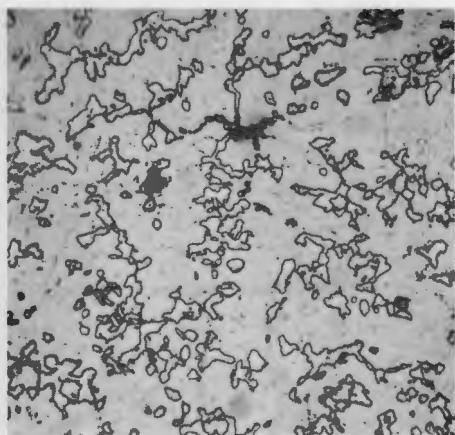


Fig. 46--52 per cent vanadium. Quenched from 900°C. Same as Fig. 45 except finely divided γ has disappeared, leaving only crystals of γ in the δ matrix. Etched with HF-HNO₃-HCl. X250.

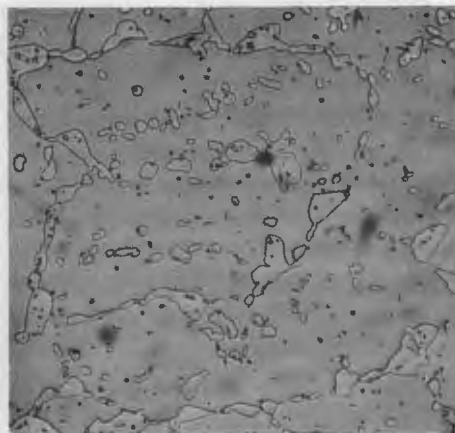


Fig. 47--52 per cent vanadium. Quenched from 1100°C. Same as Fig. 46. γ in δ matrix. Etched with HF-HNO₃-HCl. X250.

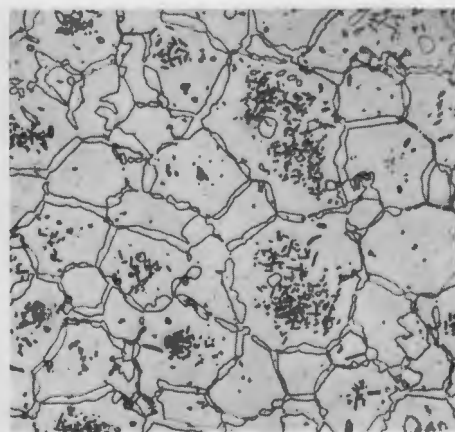


Fig. 48--50 per cent vanadium (E). Quenched from 1000°C. γ at the grain boundaries and within the grains of δ . Etched with HF-HNO₃-HCl. X250.

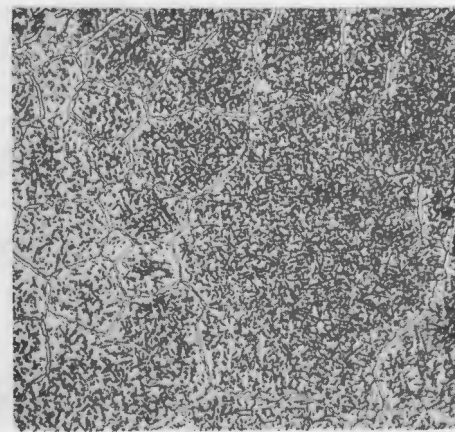


Fig. 49--48 per cent vanadium (E). Quenched from 600°C. γ at the grain boundaries and within the grains of δ . Etched with the HF-HNO₃-HCl. X250.

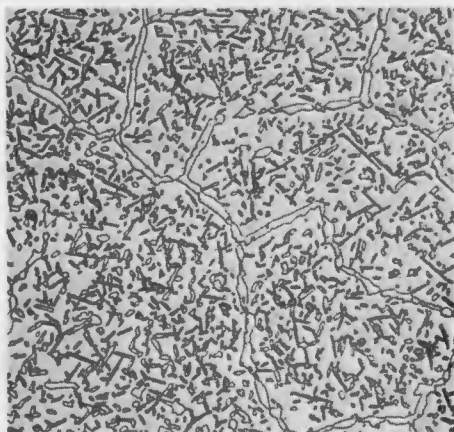


Fig. 50--48 per cent vanadium (E).
Quenched from 600°C. Higher
magnification of Fig. 49. X500.

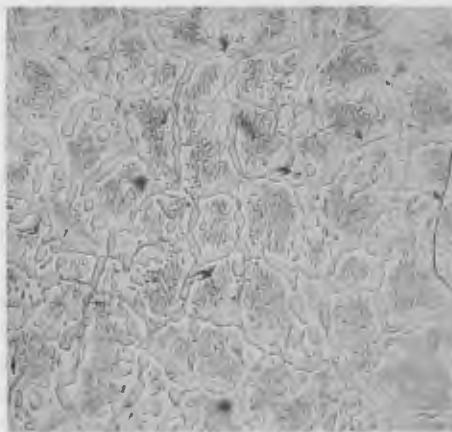


Fig. 51--47 per cent vanadium (E).
Quenched from 900°C. γ at the
grain boundaries and within the
grains of δ . Etched with HF-
 HNO_3 -HCl. X250.

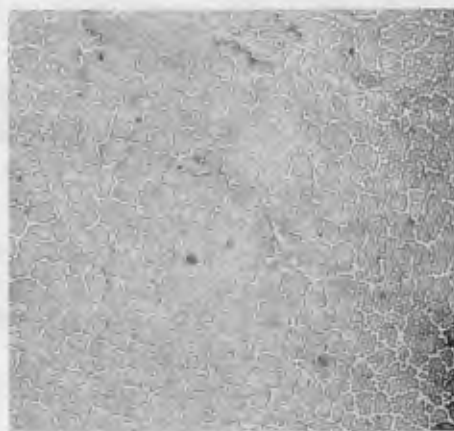


Fig. 52--46 per cent vanadium (E).
Quenched from 625°C. δ (dark) plus γ
(light). Etched with HF- HNO_3 -
HCl. X 250.

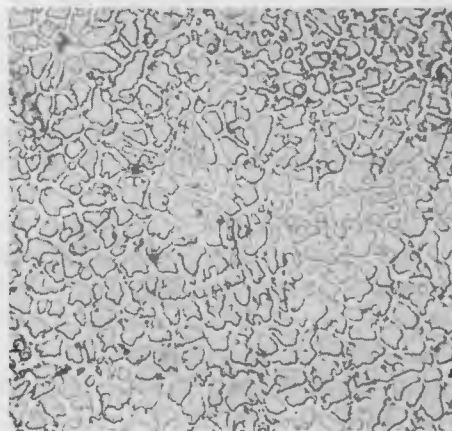


Fig. 53--45 per cent vanadium (E).
As arc-melted. Plus (continuous).
Etched with HF- HNO_3 -HCl. X250.

these three phases have been related by the two peritectic horizontals, shown in Figure 35. A thermal arrest was observed at 1360°C (Pt-Pt (10% Rh) thermocouple) in an alloy containing 37 per cent vanadium; whereas, an alloy containing 48 per cent vanadium showed neither thermal arrest nor signs of melting when heated to 1440°C. Therefore, 1360°C has been taken as the incongruent melting point of γ (Al-V).

Alloys in the range of 50 to 70 per cent vanadium were observed to become partially molten at 1670°C (optical pyrometer), and this has been taken as the incongruent melting point of δ (Al-V). Thermal data as well as other data are plotted in Figure 35.

The microstructures of the arc-melted alloys in the high aluminum portion of the system gave an early indication of still more peritectic complexities. Figure 57 shows primary dendrites of γ (Al-V) surrounded by two other phases. Partial annealing of this alloy increased its complexity, since four phases now appeared (Figure 58); the phases designated as α (Al-V) and β (Al-V) seem to have grown at the expense of γ (Al-V) and (Al), the matrix phase. That this is an approach toward equilibrium was verified by later experiments.

Thermal analysis in the range of 5 to 20 per cent vanadium showed three distinct thermal arrests at 659°C, 685°C and 735°C; 685°C and 735°C have been taken as the incongruent melting points of α (Al-V) and β (Al-V), respectively, and 659°C is the melting point of (Al). The results of the thermal analysis using chromel-alumel thermocouples, are presented in Table 7 and plotted in Figure 35. As usual, peritectic arrests are obtained with much greater clarity upon heating than upon cooling.

A series of alloys, which have been homogenized at various temperatures and then quenched, serves to illustrate the reactions which occur in high aluminum regions of the system. A 36 per cent alloy remains essentially unaltered up to 710°C (Figures 59 and 60); upon crossing the peritectic decomposition temperature (735°C) of β (Al-V), the alloy shows signs of melting (Figure 61). There is a radical change in the shape and the relative amount of γ upon crossing the 735°C horizontal since β decomposes to give liquid plus more γ . Upon further heating, the alloy continues to melt and the grains of γ grow quite large (Figure 62); also, the solubility of γ (Al-V) in the melt increases at higher temperatures, as shown by the change in the ratio of γ to liquid between Figures 61 and 62.

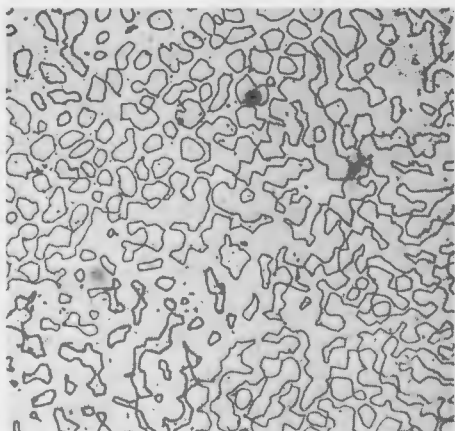


Fig. 54--45 per cent vanadium (E).
Quenched from 1100°C. δ plus γ .
Etched with HF-HNO₃-HCl. X250.

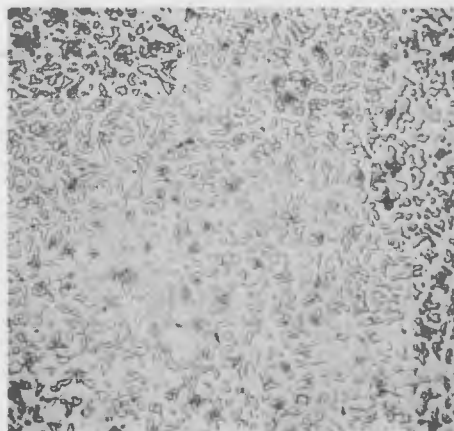


Fig. 55--43 per cent vanadium.
Furnace cooled from 800°C.
 γ (continuous, matrix) plus δ .
Etched with HF-HNO₃-HCl. X250.

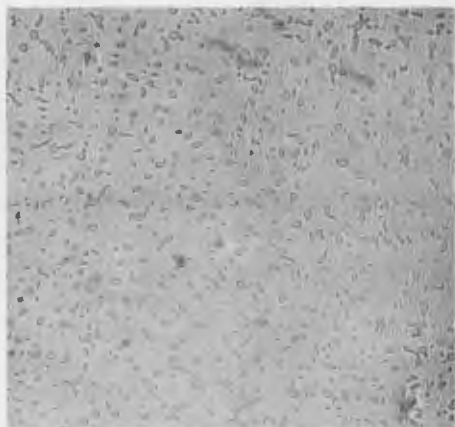


Fig. 56--42.7 per cent vanadium.
Quenched from 900°C. Small crystals of δ in γ matrix. Etched with HF-HNO₃-HCl. X250.

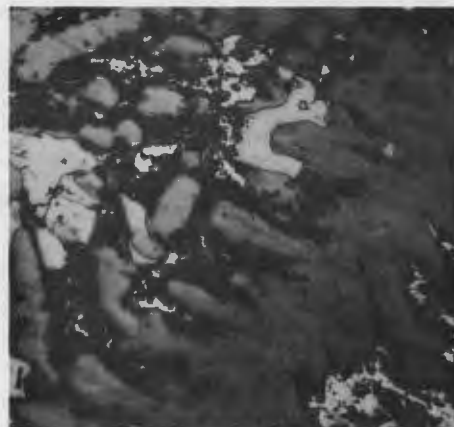


Fig. 57--19 per cent vanadium. As arc-melted. Primary dendrites of γ (grey) with β (white patches) with (Al) matrix. Etched with KOH. X500.

Table 7

Thermal Analysis with Chromel-Alumel Thermocouple

M.P. °C Comp.	(Al)		α (Al-V)		β (Al-V)	
	Heating	Cooling	Heating	Cooling	Heating	Cooling
4%V	663				737	
	662		694		737	
	662	658	694	682	732	
	658		696		735	
10%V		658	686	679	737	
	660	658	684	681	732	
	660		686		737	
	662	660	696	681	739	
18%V		661 ^a	688	684	733	
22%V		662 ^a	694	683	726	
			692	677	726	
			694		726	
39%V						

^a Alloy thought to show a pseudo-thermal arrest due to peritectic reaction.

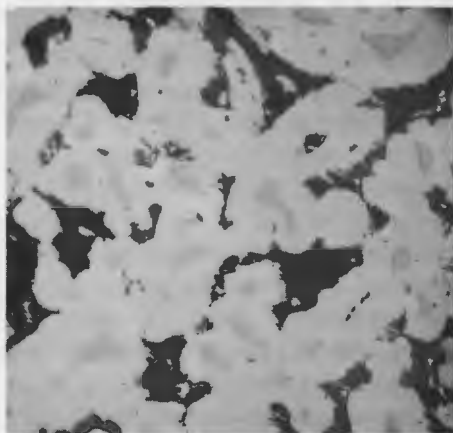


Fig. 58--19 per cent vanadium. Annealed 75 hours at 600°C and furnace-cooled. γ (grey) plus β (light grey) plus (Al) (gouged and pitted). Occasional white patch is α . Etched with KOH. X500.

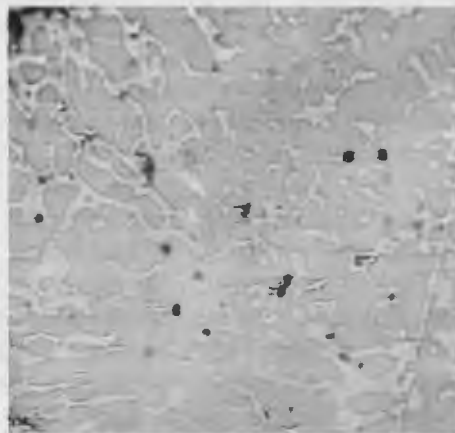


Fig. 59--36.3 per cent vanadium. Quenched from 625°C. γ (dark) plus β . Etched with HF-HNO₃-HCl. X250.

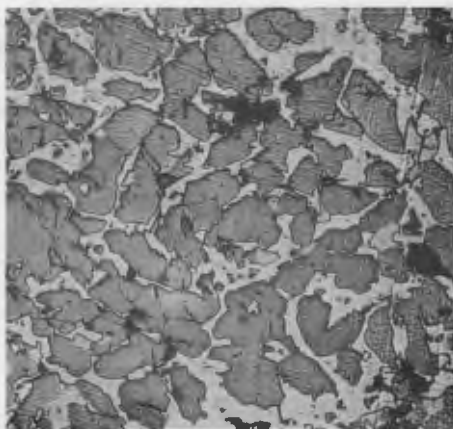


Fig. 60--36.3 per cent vanadium. Quenched from 710°C. γ (dark) plus β . Etched with HF-HNO₃-HCl. X250.

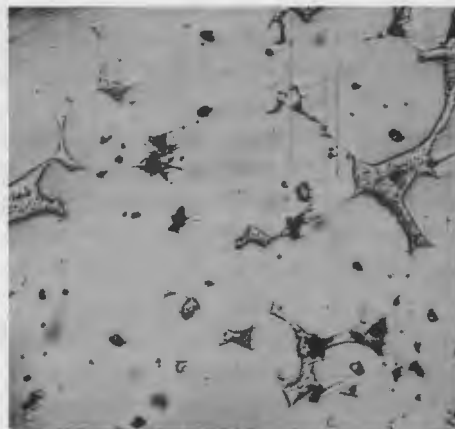


Fig. 61--36.3 per cent vanadium. Quenched from 800°C. γ plus quenched liquid (rough). Etched with HF-HNO₃-HCl. X250.

A similar sequence occurs for a 32 per cent alloy (Figures 63 and 64); and an alloy containing 27 per cent vanadium shows that β (Al-V) is completely decomposed at 750°C (Figures 65 and 66). Finally, the radical difference between Figure 16 and Figure 67 leaves little doubt that the thermal arrest observed at 735°C is associated with the incongruent melting point of β (Al-V).

Alloys containing α (Al-V) and β (Al-V) start to melt at 685°C and show only γ (Al-V) plus melt at 750°C (See Figures 68, 69, and 70). In lieu of testing the samples under polarized light, γ (Al-V) and β (Al-V) may be easily distinguished by observing that crystals of β (Al-V) retain their sharp corners when in equilibrium with the melt while crystals of γ (Al-V) become spherodized. In this regard, the sequence shown in Figures 71, 72 and 73 gives further evidence; the profiles in Figure 72 strongly suggest a random orientation of single crystals with a definite geometrical form. When the aluminum matrix of this sample was dissolved in NaOH, these crystals were indeed found to be hexagonal prisms with well-defined faces; one of the more perfect specimens was mounted for the space group determination of β (Al-V) reported below.

The series of quenches performed on the 6.3 per cent alloy shows no deviation from the pattern already established (Figures 14, 74 and 75). Many other samples were examined in this region and throughout the entire system, but since they provide only complementary information it was not thought necessary to present them here. In all, 235 samples were examined under the microscope and of these 67 were verified by X-ray analysis. The results of the thermal, microscopic and X-ray investigations on aluminum-vanadium alloys are in good agreement. A summary of the X-ray and thermal data is presented in Figure 35 against a backdrop of what is to be the proposed phase diagram for the system.

C. Atomic Nature of the System

1. Introduction

The discussion of the nature of the system on the atomic scale is likely to be the most nebulous of all since the path what is measured to what is reported is quite devious. However, information about crystal structure is often closely related to the microscopic and macroscopic

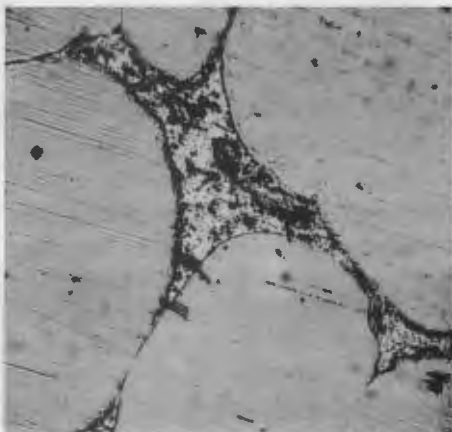


Fig. 62--36.3 per cent vanadium. Quenched from 1100°C. γ plus quenched liquid (rough). Etched with HF-HNO₃-HCl. X250.

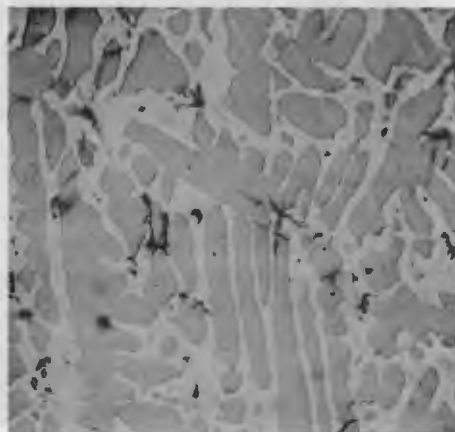


Fig. 63--32.7 per cent vanadium. Quenched from 625°C. γ (dark) plus β . Etched with HF-HNO₃-HCl. X250.

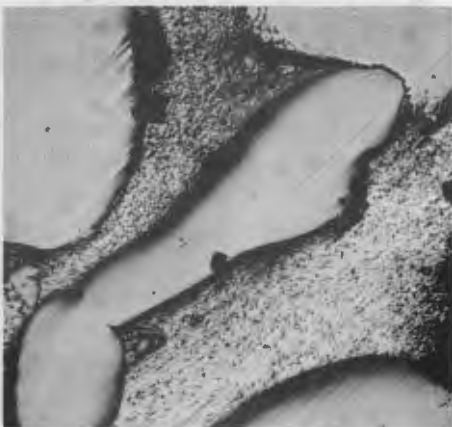


Fig. 64--32.7 per cent vanadium. Quenched from 1100°C. γ plus quenched liquid (rough). Etched with HF-HNO₃-HCl. X250.

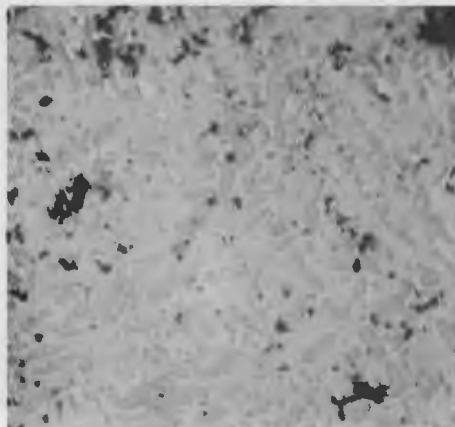


Fig. 65--27.2 per cent vanadium. Quenched from 625°C. γ (dark) plus β . Etched with HF-HNO₃-HCl. X250.

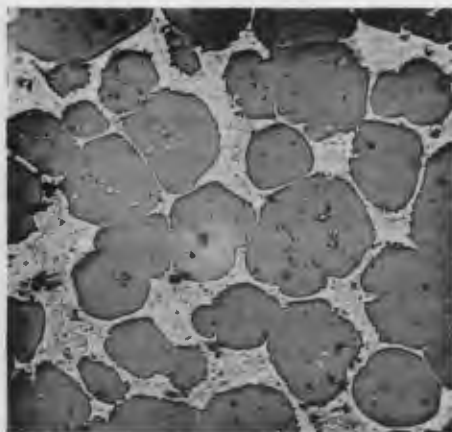


Fig. 66--27.2 per cent vanadium. Quenched from 750°C. γ (dark) plus quenched liquid. Etched with HF-HNO₃-HCl. X250.

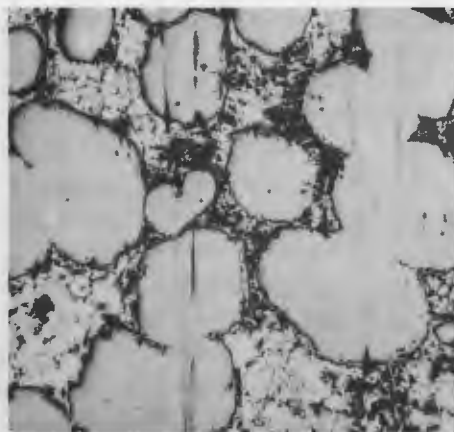


Fig. 67--23.8 per cent vanadium. Quenched from 750°C. γ plus quenched liquid (rough). Unetched. X250.

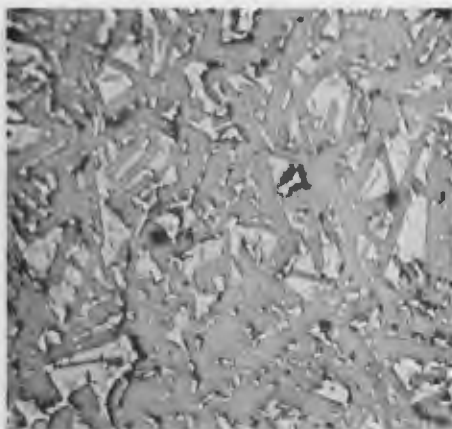


Fig. 68--17.7 per cent vanadium. Quenched from 625°C. β (light) plus . Etched with HF-HNO₃-HCl. X250.

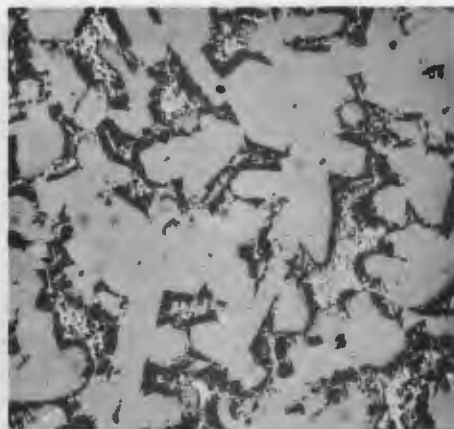


Fig. 69--17.7 per cent vanadium. Quenched from 710°C. β plus quenched liquid (rough). Etched with HF-HNO₃-HCl. X250.

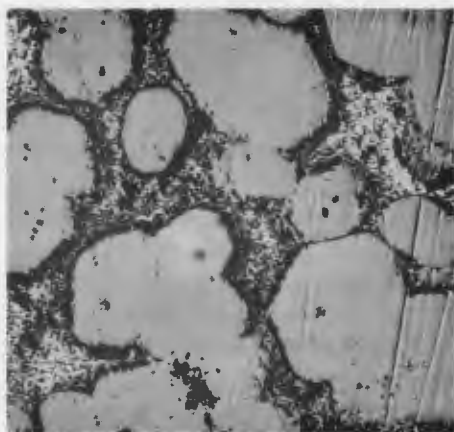


Fig. 70--17.7 per cent vanadium. Quenched from 750°C. γ plus quenched liquid (rough). Etched with HF-HNO₃-HCl. X250.

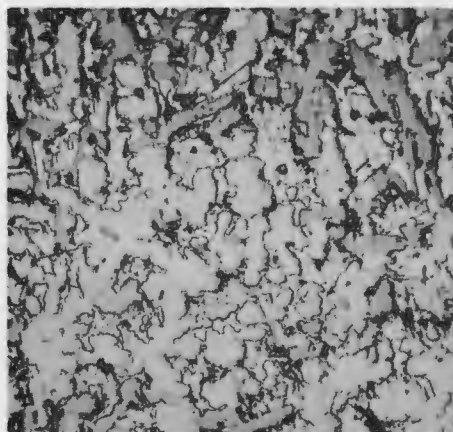


Fig. 71--10.1 per cent vanadium. Quenched from 625°C. α (smooth) plus (Al). Etched with KOH. X250.

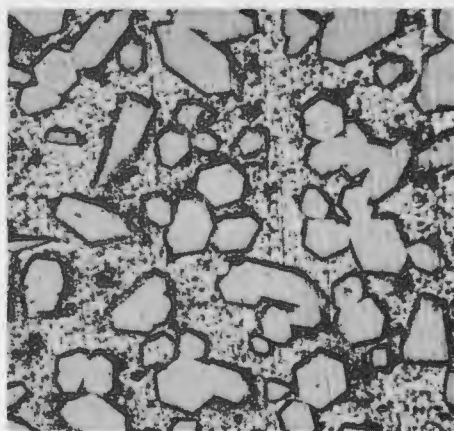


Fig. 72--10.1 per cent vanadium. Quenched from 710°C. β plus quenched liquid (rough). Etched with HF-HNO₃-HCl. X75.

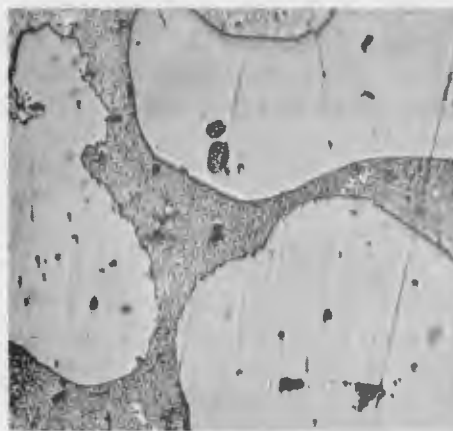


Fig. 73--10.1 per cent vanadium. Quenched from 750°C. γ plus quenched liquid (rough). Etched with HF-HNO₃-HCl. X250.

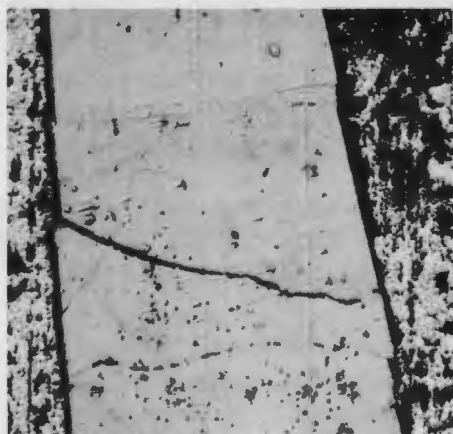


Fig. 74--6.3 per cent vanadium.
Quenched from 710°C. Large crystal of β in quenched liquid.
Etched with HF-HNO₃-HCl. X250.

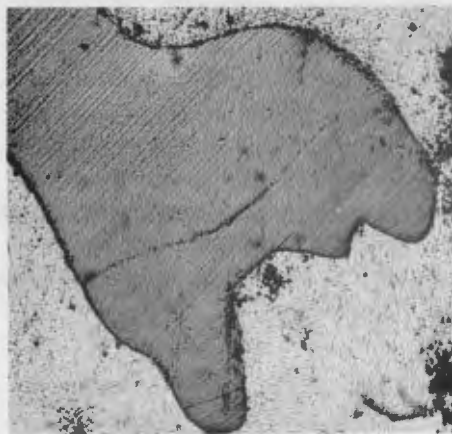


Fig. 75--6.3 per cent vanadium.
Quenched from 750°C. Large crystal of γ in quenched liquid.
Etched with HF-HNO₃-HCl. X250.

properties of an alloy. Hence it is profitable to examine the entire system again: this time from the viewpoint of atomic arrangements.

It would not be practical in the present investigation to determine the exact configuration of each atom in each phase since this requires a large amount of time and a high degree of specialization. However, surveying the system as a whole gives one advantage that is not always available to a crystallographer: a basic relation exists between the structure of a phase and its neighboring phases. Some of the coordinating links between neighboring phase structures are: substitutional solid solution, nucleation and grain growth, diffusion, and the application of Brillouin zone theory to phase structure (34).^a

Therefore, it is the purpose of this section to first describe what is known about the individual phases and then to synthesize a probable transition mechanism from one phase to the next.

In estimating the number of atoms per unit cell from the measured density, the following formula will be used:

$$n = \frac{DVA}{W}$$

where n = number of atoms per unit cell

D = density

V = volume of the unit cell

A = Avogadro's number

W = average atomic weight of the density specimen.

When an alloy containing 10 to 30 per cent vanadium is slowly cooled from 900°C in vacuo, it develops a troublesome porosity either from evaporation of aluminum or shrinkage

^aIn making an X-ray investigation of the Al-Cr system, Bradley and Lu (35) found nine intermediate phases. The powder patterns of each of the phases were remarkably similar in that the strong lines of one pattern could be almost superimposed on each of the others. Bradley commented on this situation by saying that phase formation cannot be expected to entail any great rearrangement of the atoms in the neighboring phases.

upon freezing. Although such an alloy is often unsuitable for the determination of microstructure or physical properties, it lends itself nicely to single crystal work. The surface of a vacuum-cast alloy in this percentage range is covered with a grey powder containing many sparkling points which resolve under a low-powered microscope into well-formed single crystals. Because of the peritectic complexities already described, it is possible to have many phases in a slowly cooled alloy. Hence, the phase to which a single crystal corresponded could not be deduced from the over-all composition of the alloy. No single crystals of (Al-V) were available. Crystals of α (Al-V) and δ (Al-V) were obtained from a slowly cooled casting, and a crystal of β (Al-V) was isolated from a microstructure specimen (see Fig. 72) by chemical means.

(a) δ (Al-V). The most plentiful type of crystal to be found in slowly cooled castings of 10 to 30 per cent vanadium is a long, regular, quadrangular prism. These crystals usually occur in dendrites or pine-needle clusters from which they may be separated with tweezers. Full rotation of a typical specimen in $\text{CuK}\alpha$ radiation showed these crystals to be Al_3V . This compound, as determined by Brauer (13, p. 210), belongs to space group $\text{D}_{4h}^{17} - \text{F}4/\text{mmm}$ and a structural model is shown in Figure 76. The best lattice constants available from Table 5 are $a_0 = 5.3434 \text{ \AA}$ and $c_0 = 8.3257 \text{ \AA}$ (face-centered tetragonal cell). The atomic positions are as follows:

$$4 \text{ V} \quad \text{at } 000; \frac{1}{2} \frac{1}{2} 0; \frac{1}{2} 0 \frac{1}{2}; 0 \frac{1}{2} \frac{1}{2}$$

$$4 \text{ Al} \quad \text{at } 00 \frac{1}{2}; \frac{1}{2} \frac{1}{2} \frac{1}{2}; \frac{1}{2} 00; 0 \frac{1}{2} 0;$$

$$8 \text{ Al} \quad \text{at } \pm (\frac{1}{4} \frac{1}{4} \frac{1}{4}); \pm (\frac{3}{4} \frac{3}{4} \frac{1}{4}); \pm (\frac{3}{4} \frac{1}{4} \frac{3}{4}); \pm (\frac{1}{4} \frac{3}{4} \frac{3}{4}).$$

The distance of closest approach both for Al-V and Al-Al is 2.67 \AA ; therefore the aluminum and vanadium atoms in Figure 76 and all other structure models are drawn with the same relative size. Then, too, the problem of structure determination often resolves itself into the packing of idealized, hard-shell spheres in a polyhedron on a trial and error basis. Hence, a knowledge of the size of the spheres eliminates many of the possible arrangements, and 2.67 \AA will be adopted as the best working approximation for the diameter of the aluminum and vanadium spheres.

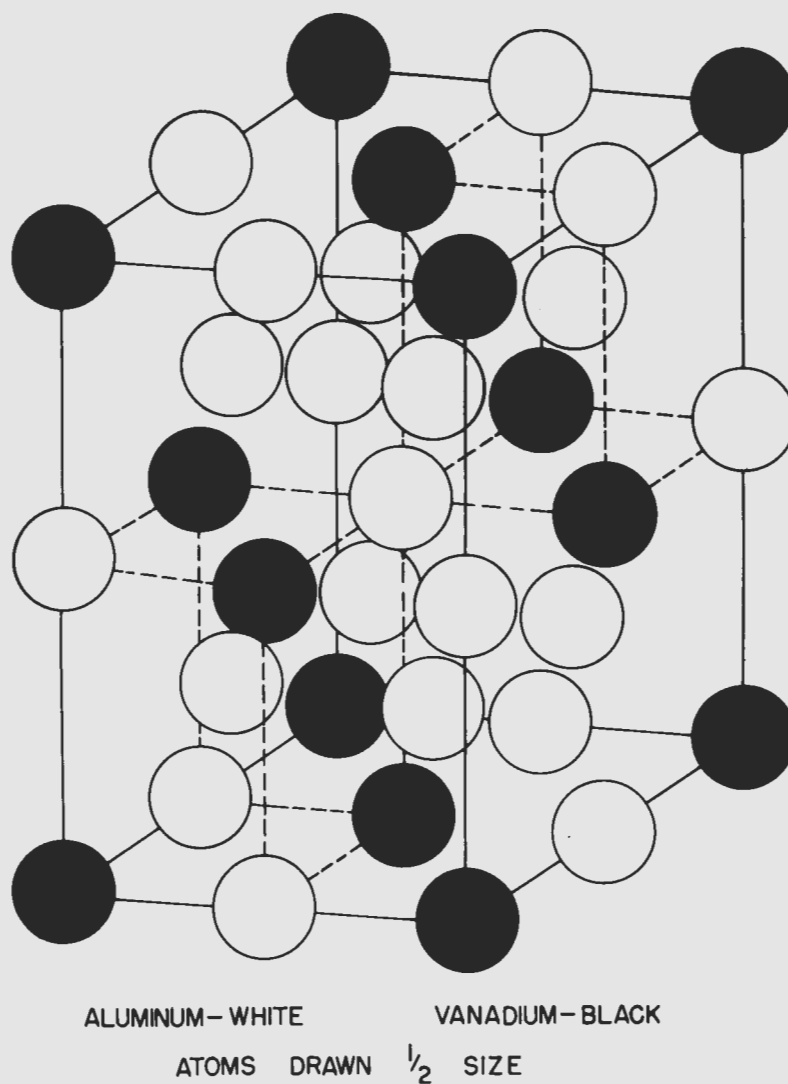


Fig. 76 - Structure Model of Al_3V

The measured density of 3.571^a for Al_3V gives 16.01 atoms per unit cell. This was already known from the structure determination, but it gives confidence in the use of density in determining atoms per unit cell.

(b) $\alpha(\text{Al-V})$. After much probing in a high-aluminum casting which was slowly cooled in vacuo, a small octahedral crystal was isolated and mounted so that one of its long axes was parallel to the axis of rotation of the goniometer. Oscillation and rotation pictures showed that this crystal was face-centered cubic with $a_0 = 14.5 \text{ \AA}$. The following systematic absences were noted in the full-rotation picture:

$(h \ k \ 0)$ except for $h + k = 4n$.

$(h \ h \ \ell)$ with $h + \ell = 2n + 1$.

The space group is, therefore, either $T_h^4 - \text{Fd}3$ or $O_h^7 - \text{Fd}3m$. Careful inspection of oscillation photographs showed that the axis of rotation had only a two-fold symmetry, and on this basis, $T_h^4 - \text{Fd}3$ has been taken as the correct space group. However, nothing could be determined about the chemical composition of the crystal without quantitative intensity data.

During the course of a liquidus experiment, however, a small piece of vanadium was inadvertently allowed to sit in a crucible of molten aluminum for several days and afterwards it was found that the vanadium had completely reacted with the aluminum. The contents of the crucible were dissolved in concentrated sodium hydroxide, and the only residue was a small homogeneous pellet (3 grams) that was neither aluminum nor vanadium. This pellet was crushed, and the X-ray pattern indexed as a face-centered cubic cell with a precision lattice constant of 14.586 \AA . Chemical analysis of this material showed the pellet to contain about 12 per cent vanadium. In other words, the small octahedral crystal was now pinned to a definite portion of the alloy system: the $\alpha(\text{Al-V})$ phase which was described in the microscopic nature of the system as being optically inactive under polarized light.

The number of atoms in a unit cell could now be determined from the densities of alloys in the range of 12 per cent vanadium. An important restriction is that the number of atoms per unit cell must be some multiple of four since the cell is face-centered cubic:

^a Interpolated from Figure 9.

<u>Wt % V</u>	<u>at % V</u>	<u>Density</u>	<u>Average At. Wt.</u>	<u>n(calc.)</u>
10.1	5.61	2.867	28.31	189.0
14.3	8.09	2.933	28.91	189.5

Therefore, there are either 188 or 192 atoms per unit cell, and there are only a few possible formulae for each case. A cell with 192 atoms means 48 atoms per molecule and 48 atoms can only be divided up into 44 Al and 4 V or 45 Al and 3 V. Everything else is outside of a reasonable composition range. Again, 188 atoms per cell means 47 atoms per molecule; 47 atoms can only be divided up in 44 Al and 3 V or 43 Al and 4 V. Thus there are only four possible formulae, and all but one of these are not allowed by the space group, $T_h^4 - Fd3$. That is, symmetry considerations will permit only the molecule containing 44 aluminum atoms and 4 vanadium atoms. Hence, (Al-V) must be $Al_{11}V$ (simplest ratio) with 192 atoms per unit cell.

There are theoretically 33 different ways of arranging 176 aluminums and 16 vanadium in $T_h^4 - Fd3$. However, packing considerations and rough intensity estimations will permit only the arrangement shown in Figure 77. The 16 vanadium atoms occur in a tetrahedron of tetrahedrons; the atomic positions being:

$$(000; \frac{1}{2} \frac{1}{2} 0; 0 \frac{1}{2} \frac{1}{2}; \frac{1}{2} 0 \frac{1}{2}) +$$

$$\frac{1}{8} \frac{1}{8} \frac{1}{8}; \frac{3}{8} \frac{3}{8} \frac{1}{8}; \frac{3}{8} \frac{1}{8} \frac{3}{8}; \frac{1}{8} \frac{3}{8} \frac{3}{8}.$$

Inside of each tetrahedron of vanadium atoms is a smaller tetrahedron of aluminum atoms. This grouping accounts for 32 aluminum atoms, since the smaller tetrahedron is also repeated in the four corners of the unit cell not occupied by vanadium tetrahedrons. The atomic positions for the eight aluminum tetrahedrons are:

$$(000; \frac{1}{2} \frac{1}{2} 0; \frac{1}{2} 0 \frac{1}{2}; 0 \frac{1}{2} \frac{1}{2}) +$$

$$xxx; x\bar{x}\bar{x}; \bar{x}x\bar{x}; \bar{x}\bar{x}x; \frac{1}{4} - (xxx; x\bar{x}\bar{x}; \bar{x}x\bar{x}; \bar{x}\bar{x}x);$$

where $x \approx 0.35$ (packing considerations).

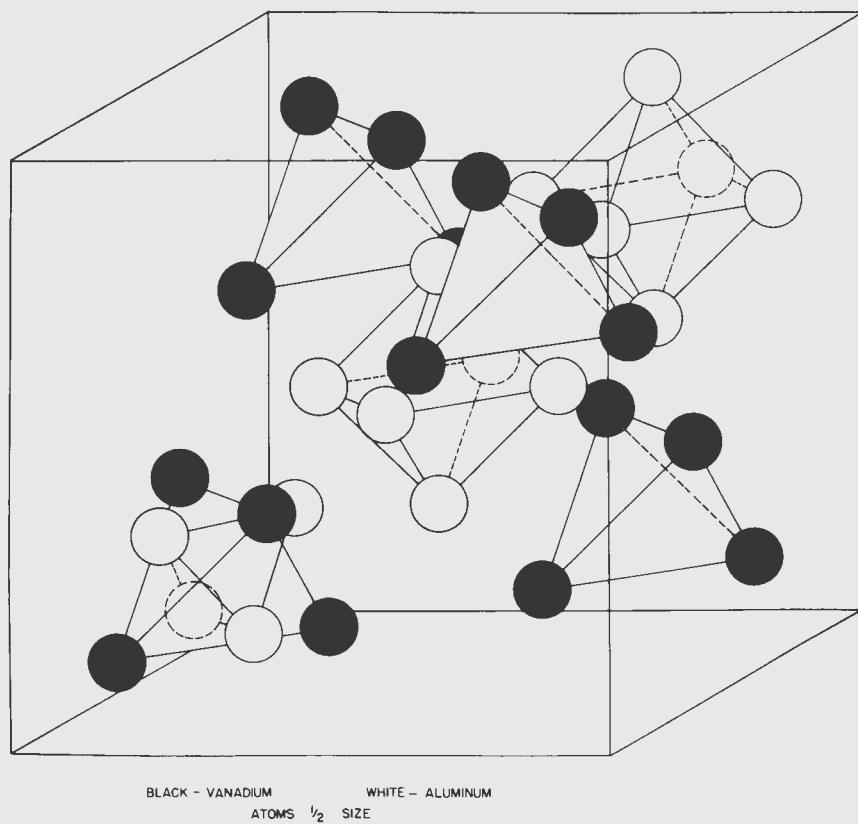


Fig. 77 - Structure Model of Al_{11}V

The four corners of the unit cell not occupied by vanadium tetrahedrons have octahedrons of aluminum atoms associated with the aluminum tetrahedrons. In addition, there is an aluminum octahedron at the center of the unit cell, which is repeated at the center of each of the twelve edges of the unit cell giving a face-centered array. These two groupings of octahedrons account for 48 aluminum atoms whose positions are:

$$\begin{aligned} & (000; \frac{1}{2} \frac{1}{2} 0; \frac{1}{2} 0 \frac{1}{2}; 0 \frac{1}{2} \frac{1}{2}) + \\ & \pm(x00; 0x0; 00x); \frac{1}{4} \pm(x00; 0x0; 00x); \end{aligned}$$

where $x \approx 0.30$ (packing considerations).

In addition, there are 96 aluminum atoms not represented in Figure 77 with atomic positions involving three unknown parameters.

(c) β (Al-V). As mentioned above in the section on microstructures, a 23.8 per cent alloy showed one phase which was optically active. Then too, it was possible to isolate and mount a well-formed crystal of this anisotropic or β phase. The lattice constants were measured on a Buerger precession camera with Mo $K\alpha$ radiation; the crystal was found to be hexagonal with $a_0 = 7.718 \text{ \AA}$ and $c_0 = 17.15 \text{ \AA}$. Precession and Weissenberg pictures of the reciprocal space lattice about c_0 gave $C6_l$ symmetry at all levels. The Laue symmetry is thus $D6_h$. The following systematic extinctions were noted:

$$\begin{aligned} (hk\ell) & \text{ none} \\ (hh\ell) & \text{ with } \ell = 2n. \end{aligned}$$

Therefore, the possible space groups are $D6_h^4 - C6/mmc$, $C6_v^4 - C6mc$ or $D3^4 - C62c$. For these space groups the number of atoms per unit cell must be some multiple of two.

The density (3.072) of the 23.8 per cent vanadium alloy gave 55.5 atoms per unit cell. This in turn gave only one possible formula that was permitted by the space groups: Al_6V with 56 atoms per unit cell.

Unlike the situation for α (Al-V), a unique packing arrangement could not be determined for this structure on the basis of steric hinderance or qualitative intensities. Quantitative intensity measurements and the resulting Patterson vectors should give more structural information.

(d) $\sqrt{\text{Al-V}}$. The microscopic investigation showed that an isotropic one-phase region existed near 56 per cent vanadium. The X-ray powder photographs of alloys in this range indexed as a body-centered cubic cell with $a_0 = 9.207 \text{ \AA}$. Density measurements on several alloys in this region gave approximately 53 atoms per unit cell which meant that the cell actually contained either 52 or 54 atoms. (Body-centered cells contain two molecules). Since single crystal data were not available, no unique space group determination could be made. However, it was known that the structure must conform to some sort of a super lattice since a_0 was exactly three times as long as a_0 for (V), and the strong lines of $\sqrt{\text{Al-V}}$ were the body-centered lines of (V). That is, the (110) line of (V) was the (330) line of $\sqrt{\text{Al-V}}$.

A survey of the literature suggested that $\sqrt{\text{Al-V}}$ belonged to the γ -Brass type of structure of which there are 32 known representatives. The cell contains 52 atoms and belongs to the space group $T_d^3 - I43m$. Symmetry considerations will permit only three possible formulae: Al_9V_4 , Al_8V_5 , and Al_7V_6 . Al_7V_6 and Al_9V_4 seem to be almost outside of a reasonable composition range, but there is no justification for assuming that the theoretical formula composition must fall within the one phase region. Then too, Al_9V_4 might be isomorphous with Al_4Cu_9 , and Al_7V_6 is theoretically favorable since it has an electron to atom ratio of 21 to 13.

Intensity calculations have been made for the possible formulae in order that a unique formula may be chosen by comparison with the relative intensities of a powder photograph. The results are shown in Table 8. The space group permits two possible arrangements of Al_8V_5 ; the primed formula corresponds to the arrangement shown by Al_8Cr_5 ; which has a distorted γ -Brass structure (33, p. 30), and the unprimed formula corresponds to the arrangement of the Zn_8Ag_5 . The structure that is isomorphous with Zn_8Ag_5 gives the best fit to the observed powder intensity of a 58 per cent vanadium alloy.^a For the sake of comparison, the powder intensity of Zn_8Ag_5 (36) is included.

The slightly idealized structure of $\sqrt{\text{Al-V}}$ is shown in Figure 78. The atomic positions are:

^aThe numerical intensities shown have been calculated by an approximation method used by Bradley and Thewlis (32, p. 684) in the original structure determination of γ -Brass. A vanadium atom has approximately 1.8 times the scattering power of an aluminum atom. A numerical intensity substantially greater than 1.0 should correspond to a line on the film, however weak.

Table 8
Intensity Calculations for $\sqrt{\text{Al-V}}$

	Zn ₈ Ag ₅ 58%V		Al ₇ V ₆	Al ₈ V ₅	Al ₉ V ₄	Al ₈ V ₅ '
110	X	VVW	0.5	2.9	34.5	15.4
200	X	X	3.4	0.5	0.6	0.2
211	VW	VW	4.0	18.9	7.2	3.8
220	X	X	3.3	1.0	0.2	0.4
310	X	X	1.2	0.9	4.1	2.4
222	W	VVW	23.9	1.6	5.8	10.1
321	X	VVW	27.8	1.3	4.6	7.5
400	X	X	1.0	0.0	2.7	0.6
411, 330	S	VS	193.0	218.0	164.0	190.0
420	X	X	0.3	0.0	0.0	0.1
332	W	W	19.3	9.8	23.5	26.2
422	W	M	19.8	36.5	44.7	43.5
510, 431	VW	VW	11.3	2.2	14.6	10.8
521	X	X	17.1	1.4	2.1	0.1
440	W	X	1.3	0.5	4.3	1.6
530, 433	X	X	14.2	0.7	1.6	4.6
600, 442	S	M	17.7	35.1	12.7	16.7
611, 532	W	VW	8.1	10.4	7.0	13.3
620	X	X	0.1	0.2	0.8	0.9
541	VW	VVW	2.2	6.8	4.1	0.1
622	X	X	7.0	0.4	0.2	0.4
631	W	W	22.7	7.8	16.9	12.5
444	M	W	26.7	19.3	16.9	18.3
710, 550, 543	W	W	28.9	19.3	22.2	25.5
640	X	X	1.9	0.6	5.5	0.2
633, 721, 552	S	S	61.5	91.6	68.1	71.2
642	X	VW	7.7	2.9	6.4	5.4
730	X	X	2.9	0.6	2.3	0.1
651, 732	X	VW	20.2	10.0	22.6	20.0
800	X	X	0.5	0.3	1.5	0.0
811, 741, 554	S	M	48.7	46.6	40.1	38.0
820, 644	W	VW	3.5	6.0	4.2	3.4
653	X	VVW	4.8	1.6	3.3	2.4
822, 660	M	M	21.7	25.2	25.8	23.8

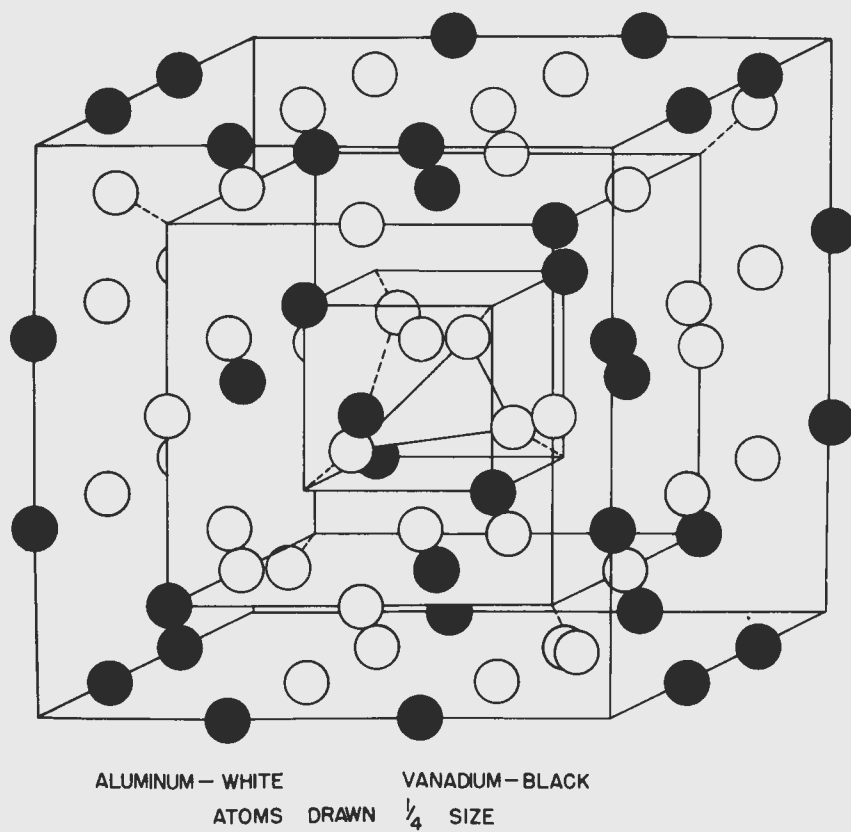


Fig. 78 - Structure Model of Al_8V_5

8 V at $(000; \frac{1}{2} \frac{1}{2} \frac{1}{2}) + xxx; x\bar{x}\bar{x}; \bar{x}x\bar{x}; \bar{x}\bar{x}x$; where $x = \frac{1}{6}$;

8 Al at $(000; \frac{1}{2} \frac{1}{2} \frac{1}{2}) + xxx; x\bar{x}\bar{x}; \bar{x}x\bar{x}; \bar{x}\bar{x}x$; where $x = 0.36$;

12 V at $(000; \frac{1}{2} \frac{1}{2} \frac{1}{2}) \pm (x00; 0x0; 00x)$; where $x = 0.36$;

24 Al at $(000; \frac{1}{2} \frac{1}{2} \frac{1}{2}) + xxz; zxx, xzx; x\bar{x}\bar{z}; z\bar{x}\bar{x}; x\bar{z}x;$
 $\bar{x}x\bar{z}; \bar{z}x\bar{x}; \bar{x}z\bar{x}; \bar{x}\bar{x}z; \bar{z}\bar{x}x; \bar{x}\bar{z}x;$

where $x = 0.31$; $z = 0.045$.

2. Phase transitions

The structure of γ and $\sqrt[3]{}$ can be visualized as evolving from the solid solution phase, (V). When an aluminum atom is substituted at random in the body-centered vanadium lattice, it tends to surround itself with certain preferred nearest neighbors. All substitutional solid solutions exhibit, to a greater or lesser degree, this tendency, which is sometimes referred to as short-range ordering. If aluminum preferred eight nearest vanadium neighbors, it would almost certainly undergo long range ordering or compound formation at 50 atomic per cent aluminum.^a This does not happen in this system (even in spite of the favorable electron to atom ratio of 3 to 2) because aluminum prefers four nearest vanadium neighbors and four nearest aluminum neighbors arranged tetrahedrally. Hence if the $\sqrt[3]{}$ phase did not form, the solid solution would almost certainly undergo long-range ordering or compound formation by the time that there were three aluminums for every vanadium. Indeed, Figure 76 shows that γ (Al-V) is really a distorted super-lattice with aluminum in the center of a small cube and aluminum and vanadium sharing tetrahedral corners; the whole lattice has been stretched in the z direction because every other (o o l) plane contains only aluminum atoms.

$\sqrt[3]{}$ (Al-V) may then be looked upon as an intermediate structure between (V) and γ . Actually as the atomic concentration approaches 50 per cent aluminum, the solid solution lattice undergoes long-range ordering; a large cube of 27 (V) cubes is formed which then loses 2 of its 54 atoms. One aluminum from the center and each of the eight

^a This actually happens in the aluminum-titanium system (31, p. 613) where the β -Brass type of super-lattice is formed with an aluminum in the center of a cube and titanium at each of the eight corners.

corners of the large cube is lost, and the atoms rearrange slightly to relieve the strain caused by the vacancies (see Fig. 78).

It is significant that the small cube in the center of Figure 78 is exactly the structural kernel that occurs in α (Al-V): a small tetrahedron of aluminums associated with a larger tetrahedron of vanadiums (see Fig. 77). The octahedrons of aluminums in Figure 77 can be thought of as the remains of the face-centered (Al) lattice which has been distorted in the formation of the giant unit cell of α (Al-V).

Unfortunately, sufficient structural information concerning β (Al-V) has not been obtained to determine even the positions of the vanadium atoms and no comparisons can be made with its neighboring structures.

VII. DISCUSSION AND SUMMARY

The binary alloy system of aluminum and vanadium has been investigated by thermal, microscopic, chemical and X-ray methods. Density and a few of the other physical properties are reported. In general, thermal, microscopic and X-ray data are in good agreement concerning the nature of the alloy system; however, an uncertainty in chemical composition was introduced by the difficulty in preparing homogeneous samples.

An essentially complete picture of the room-temperature phase relationships has been presented. The phase boundaries and X-ray properties of the six single-phase regions are given together with the interrelations which exist among these phases on the microscopic and atomic scales. The four intermediate phases appear to be peritectic in nature which may account for such unusual macroscopic behavior as: cold-worked alloys becoming harder upon annealing, arc-melted alloys exploding upon cooling, and cast alloys from 20 to 40 per cent vanadium being porous and friable. Also alloys between 15 and 70 per cent vanadium can be crushed to 300 mesh powder without signs of cold work.

Much of the data accumulated from this work and from reliable references is summarized by the phase diagram proposed in Figure 79. The liquidus up to 1100°C is taken from Mondolfo (14, p. 48) who reported some information on the solubility of vanadium in liquid aluminum. From 1100°C to 1800°C , the liquidus is sketched in to conform with the optical pyrometer data and the horizontals at 1360° and 1670°C .

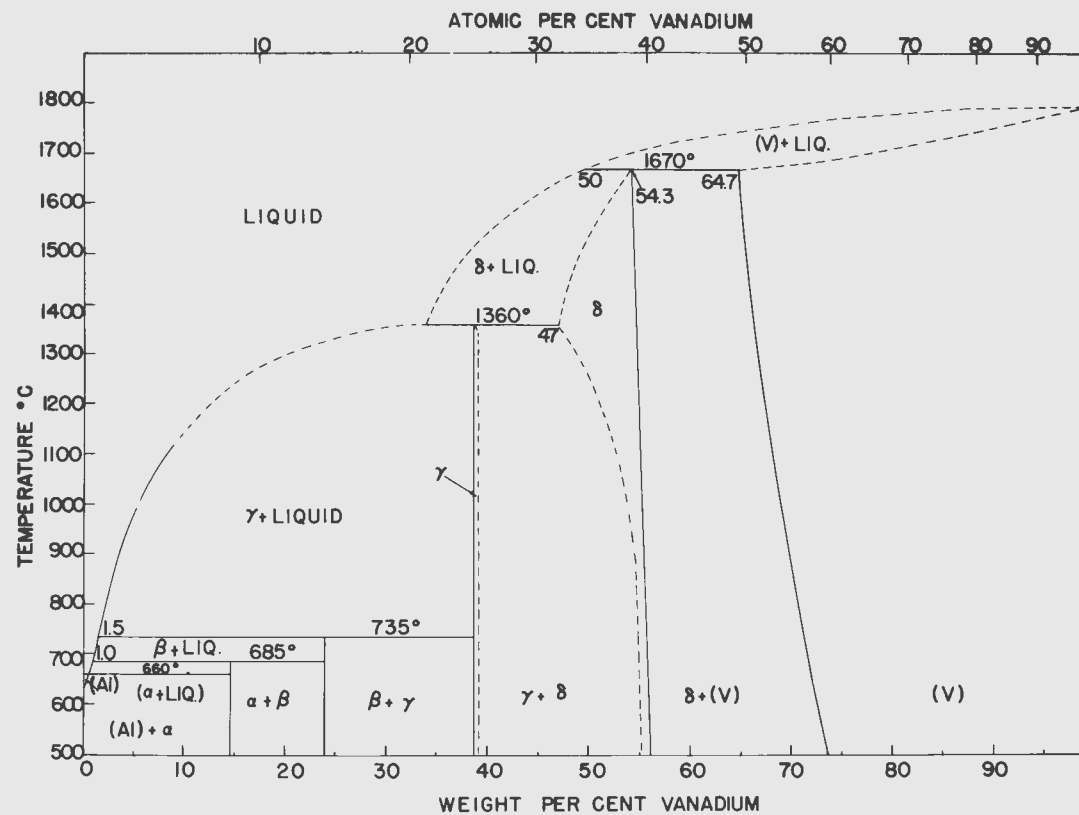


Fig. 79 - Proposed Phase Diagram for the Aluminum-Vanadium System.

The one-phase regions for α (Al-V) and β (Al-V) are represented as vertical lines for want of experimental evidence to the contrary. γ (Al-V) and δ (Al-V) have been given finite solid solubility ranges at low temperatures, but the exact extent of these solubilities is unknown. On a graph of $1/T^{\circ}\text{K}$ versus log atomic per cent, the solvus for (V) (obtained from Figure 28) gave a straight line which could be extrapolated to 1670°C . This extrapolation gave 64.7 weight per cent vanadium for the terminal solid solubility point which is in good agreement with the microstructure value of 65 per cent. One of the phase boundaries for the δ phase has been drawn with a full line to express a degree of confidence in its location. This line between δ and δ plus (V) is somewhat restricted in its location by the fact that δ (Al-V) is a super-lattice of (V).^a The phase boundary between δ and γ plus δ has been sketched in to conform with the microscopic evidence. Finally, the solvus for (Al) may be drawn according to the work of Roth (12, p. 359) or the method proposed by Fink and Freche (37); on the scale used in Figure 79, the difference between these two methods is negligible.

A survey of the system on an atomic scale provided an unambiguous formula for each of the intermediate phases. In addition, the crystal symmetry found for each phase was in good agreement with microscopic and macroscopic properties of each phase. That is, the hexagonal and tetragonal phases showed optical activity under polarized light while the cubic phase did not. Then, too, α , β and γ which were cubic, hexagonal and tetragonal, respectively, formed octahedral, hexagonal and tetragonal single crystals, respectively. Finally, a correlation of phase structure was presented which was keynoted by the preference of aluminum for four nearest vanadium neighbors and four nearest aluminum neighbors arranged tetrahedrally and also by the marked tendency toward super-lattice formation.

^aThe lattice constants of (V) in the two-phase region will be exactly one-third the corresponding lattice constants for δ (Al-V). Hence, Figure 28 has been extended to include the probable location of the phase boundary between δ and δ plus (V). If Al_{18}V_5 is the highest melting composition in δ (Al-V), the lattice constant versus composition plot for δ may be anchored at 1670°C . This plot is further restricted by the known positions of the two-phase regions from the microstructures.

VIII. LITERATURE CITED

1. Glasstone, S. and Edlund, M. C., "The Elements of Nuclear Reactor Theory", p. 58, D. Van Nostrand Co. Inc., New York, N. Y. (1952).
2. Huges, D. J., Spatz, W. D. E. and Goldstein, N., Phys. Rev., 75, 1781 (1949).
3. Seybolt, A. V., Atomic Energy Comm. Periodical TID-70: J. Metallurgy Ceramics, 6, 23 (1951).
4. Kinzel, A. B., Metal Progress, 58, 315 (1950).
5. Clarke, F. W., U. S. Geol. Survey Bull., 770, 34 (1924).
6. Matignon, C. and Monnet, E., C. R. Acad. Sci., Paris, 134, 542-45 (1902).
7. Czako, N., C. R. Acad. Sci., Paris, 156, 140-42 (1913).
8. Schirmeister, H., Stahl und Eisen, 35, 998 (1915).
9. Corson, W. C., "Aluminum, the Metal and its Alloys", D. Van Nostrand Co., New York, N. Y. (1926).
10. Fuss, V., "Metallography of Aluminum and its Alloys", p. 151-2. Translated from the German by Robert J. Anderson, the Sherwood Press, Cleveland, Ohio (1936).
11. Anonymous, Aluminum Broadcast, 3, 12-13 (1931). Original not available for examination; abstracted in J. Inst. Metals, 50, 472 (1932).
12. Roth, Albert, Z. Metallkunde, 32, 356-9 (1940).
13. Brauer, George, Z. Elektrochem., 49, 208-10 (1943).
14. Mondolfo, L. F., "Metallography of Aluminum Alloys" p. 48-49, John Wiley and Sons, Inc., New York, N. Y. (1943).
15. Clark, W. W., Trans. Am. Inst. Metals, 8, 8 (1915).
16. Hopkins, B. S., "Chapters in the Chemistry of the Less Familiar Elements", Stipes Pub. Co., Champaign, Ill. (1939).
17. Eborall, M. D., J. Inst. Metals, 76, 295-320 (1949).

18. Frary, F. C., Trans. Am. Electrochem. Soc., 47, 275 (1925).
19. American Society for Metals, "Physical Metallurgy of Aluminum Alloys". Cleveland, the Society. (1949). Twenty-eighth National Metal Congress and Exposition, Atlantic City.
20. Long, J. R., Unpublished Ph. D. Thesis, Ames, Iowa, Ames Lab. of Atomic Energy Comm. (1951).
21. Powers, R. M., Unpublished Ph. D. Thesis, Ames, Iowa, Ames Lab. of Atomic Energy Comm. (1952).
22. Pearson, W. B., J. Iron and Steel Inst., 164, 149-59 (1950).
23. McCutcheon, D. M. and Pahl, W., Metal Progress, 56, 674-9 (1949).
24. Carver, C., Metal Progress, 59, 371 (1951).
25. Cohen, M. V., Rev. Sci. Instr., 6, 68 (1935).
26. Nelson, J. B. and Riley, D. P., Proc. Phys. Soc., 57, 164 (1945).
27. Willard, H. H. and Young, P., Ind. Eng. Chem., Anal. Ed., 6, 48 (1934).
28. Telep, G. and Boltz, D. F., Anal. Chem., 23, 901-3 (1951).
29. Hartshorn, J. H., Laboratory Notebook JHH-1-41, Ames Lab. of Atomic Energy Comm. (1953).
30. Lord, J. O., "Alloy Systems", p. 313-14, Pitman Publishing Corp., New York, N. Y. (1949).
31. Bumps, E. S., Kessler, H. D. and Hansen, M., J. Metals, 4, Trans., 609-14 (1952).
32. Bradley, A. J. and Thewlis, J., Proc. Roy. Soc. (London) 112 A, 678-92 (1928).
33. Bradley, A. J. and Lu, S. S., Zeit. Krist., 96, 20-37 (1937).
34. Cottrell, A. H., "Theoretical Structural Metallurgy," p. 148-52, Edward Arnold and Co., London, England (1951).
35. Bradley, A. J. and Lu, S. S., J. Inst. Metals, 60, 319 (1937).

36. Westgren, A. F. and Phragmen, G., Phil. Mag., 50,
311-41 (1925).
37. Fink, W. L. and Freche, H. R., Trans. A. I. M. E.,
111, 304 (1934).